Journal of Molecular Graphics and Modelling 143 (2026) 109264

Contents lists available at ScienceDirect

Journal of Molecular Graphics and Modelling

journal homepage: www.elsevier.com/locate/jmgm

Computational studies of target-specific radiopharmaceuticals for theranostics

Silvia Gervasoni *, Camilla Guccione, Giuliano Malloci *

Department of Physics, University of Cagliari, Cittadella Universitaria, S.P. Monserrato-Sestu Km 0.7, Monserrato, I-09042, CA, Italy

ARTICLE INFO

Keywords:
Cancer theranostics
Radiopharmaceuticals
Structure-based drug design
Molecular docking
Molecular dynamics simulations

ABSTRACT

Radiopharmaceuticals are key tools in nuclear medicine, enabling both diagnostic imaging and targeted therapy for conditions such as cancer and neurological disorders. The integration of computational techniques in the drug-discovery process, such as molecular docking and molecular dynamics simulations, contributes to the development of this class of compounds. Here we review recent computational studies on radiopharmaceuticals acting on different targets: receptors, enzymes, and transporters. Several receptors such as chemokine receptor 4, neurokinin-1, metabotropic glutamate receptor, and gastrin-releasing peptide receptor have been investigated using molecular simulations to optimize ligand binding and enhance receptor targeting. Enzymes like prostate-specific membrane antigen and fibroblast activation protein α have been investigated *in silico* for their interaction with novel radiopharmaceutical inhibitors. Additionally, transporter proteins such as glucose transporters have been explored for their role in cancer metabolism and imaging applications. Advanced computational studies, including quantum mechanics calculations and free energy estimations, have contributed to our understanding of radiopharmaceutical binding modes and stability at the molecular level of detail. The review highlights the potential of computational approaches for cost-effective design of next-generation theranostic agents, emphasizing the importance of molecular databases in ligand-based drug discovery and artificial intelligence-based drug design.

1. Introduction

Radiopharmaceuticals are essential tools in nuclear medicine, where radioactive isotopes are combined with biological targeting agents to diagnose and treat diseases such as cancer, cardiovascular conditions, and neurological disorders [1]. These compounds provide unique insights into molecular and cellular processes according to the decay properties of the specific radionuclide associated with the drug. Radionuclides emitting γ-ray or β^+ radiations interact minimally with the tissues and are used for imaging purposes (*e.g.*, ^{68}Ga, ^{99m}Tc, ^{177}Lu), while those emitting β^- or α particles deposit high energy in the tissues and are used for therapy purposes (*e.g.*, ^{177}Lu or ^{90}Y) [2–4]. In the latter case, the radiopharmaceuticals are embedded inside the target cells, where they can act as cytotoxic factors. Radiopharmaceuticals are designed to bind to specific biomarkers, enhancing diagnosis and therapy precision [5]. One common strategy in designing radiopharmaceuticals is to conjugate a biovector with a chelator moiety that carries the radionuclide. The biovector is the portion of the compound that has high affinity for the target, while the chelator is responsible for firmly coordinating the radionuclide (Fig. 1). As a result, radiopharmaceuticals rely on the synergy between radiometals, chelators, and biovectors. The proper assembling of these components, informed by properties like oxidation state and coordination geometry, is crucial for overall stability and efficacy [6]. Furthermore, since the chelator moiety is often bulky (*e.g.*, dodecane tetraacetic acid — DOTA), a common strategy is to employ a linker that connects the two portions [7], in order not to impair biovector's activity.

The biovector of many radiopharmaceuticals is a peptide, like in the case of the marketed drug Lutathera® [8]. This specific type of targeted treatment is called peptide receptor radionuclide therapy (PRRT), and it is often used for treating neuroendocrine tumors [9,10], as well as other types of cancers [11]. In PRRT the endogenous peptide ligands of the target receptors are used as a guide to design new peptides, usually incorporating some non-standard residues to improve their half-life. Peptides are characterized by high flexibility and their 3D rearrangement (or secondary structure) is crucial for their activity. The application of computational techniques within this field of research is quite challenging due to the presence of non-standard atoms (*e.g.*, Ga, Cu, Lu, Y, At) that do not have a straightforward parameterization when using molecular mechanics (MM) force fields [12], and due

* Corresponding authors.
E-mail addresses: silvia.gervasoni@dsf.unica.it (S. Gervasoni), giuliano.malloci@dsf.unica.it (G. Malloci).

https://doi.org/10.1016/j.jmgm.2025.109264
Received 3 June 2025; Received in revised form 10 December 2025; Accepted 19 December 2025
Available online 20 December 2025

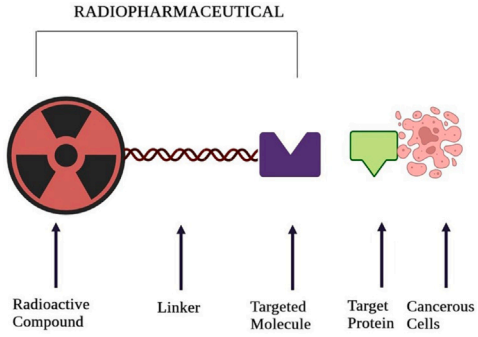

Fig. 1. Typical structure of a radiopharmaceutical compound. The biovector (targeted molecule) is associated with a radioactive compound through a linker. The biovector targets a specific protein, which is usually a hallmark of a particular disease.
Source: Reproduced with permission from Ref. [7].

to the high flexibility of the peptide portion [13,14]. Targeted radiopharmaceuticals have garnered increasing attention from clinicians and researchers due to their remarkable efficacy in cancer treatment, particularly for patients with refractory and metastatic cancers who derive limited benefit from chemotherapy and other conventional therapies. By selectively delivering cytotoxic radiation to tumor cells, while sparing healthy tissues, targeted radiopharmaceuticals offer a precision medicine approach that enhances treatment efficacy and minimizes adverse effects. Their ability to address treatment-resistant malignancies makes them a promising option for improving patient outcomes in oncology [4,7,15–17]. Computer-aided drug design (CADD) has been instrumental in improving probes for positron emission tomography (PET)/ single-photon emission computed tomography (SPECT) and radio-therapy, facilitating the rational design of new compounds with enhanced stability and reduced toxicity [14,18].

In recent years, different comprehensive reviews have been published addressing various aspects of computational approaches in radiopharmaceutical research. Salahinejad et al. [18] reported an overview of the main types of radiopharmaceuticals and their application, discussing how different computational techniques have been used for their design. Patamia et al. [14] presented an overview of applications of computational methods for the design of peptide-based PET and SPECT probes. Jackson et al. [19] focused on machine learning methodologies applied to the development of radiopharmaceuticals targeting the central nervous system, while Tao et al. [20] focused on AI in radiopharmaceutical discovery and molecular image analytics. Finally, Ataeinia and Heidari [21] described some applications of *in silico* methods for radiopharmaceutical design applied to cancer, central nervous system, infection and inflammation. Our updated review complements these prior works by specifically emphasizing structure-based computational studies across diverse molecular targets and integrating mechanistic insights with applications in diagnosis, therapy or both (theranostics). In this updated review, we aim to retrace and summarize the main studies in which CADD has been used to identify or optimize new radiopharmaceuticals for a large variety of applications. We have organized the discussion according to different target typologies, with a particular focus on receptors, enzymes, immune checkpoint markers, transporters, and disordered proteins. We briefly report on nanoplatforms and metal–organic systems, and on key databases containing radiocompounds that can be exploited as valuable sources of data for machine learning training (Table 1). Finally, we critically discuss common challenges of every target and the future perspectives. This targeted scope, combined with a focus on recent advances in molecular simulations and free energy calculations, distinguishes our contribution in the evolving landscape of computational radiopharmaceutical research.

Table 1
Summary of the works discussed in this review. HM: Homology modeling, Dock: Molecular docking, MD: Molecular dynamics simulations, QM: Quantum mechanics calculations, GaMD: Gaussian accelerated MD, FE: Free energy calculation, cDock: Covalent docking, US: Umbrella sampling, QSAR: Quantitative structure–activity relationship.

		Studies	Methods
Receptors	SSTR2	[22] [23]	HM, Dock MD
	CCK2R	[24]	HM, Dock
	GRPR	[25]	HM, MD
	DR	[26] [27]	Dock, MD, QM HM, Dock
	CXCR4	[28] [29]	Dock Dock, GaMD
	NK1R	[30]	Dock, MD
	mGluR	[31] [32]	Dock, MD HM, Dock
	HER2	[33] [34]	Dock Dock, MD, FE
	$\alpha\beta$ Integrins	[35] [36]	Dock, MD, FE Dock
	TSPO	[37]	HM, Dock
Enzymes	PSMA	[38] [39]	Dock Dock, MD
	FAP	[40] [41] [42]	Dock cDock QSAR
Immune Escape Proteins	PD-L1	[43–47] [48,49]	Dock Dock, QM
Transporters	GLUTs	[50]	Dock, MD, FE
	DAT	[51]	QSAR
Disordered Proteins	β-amyloid	[52]	QM
	α-sinuclein	[53] [54]	Dock Dock, US

2. Computational methods

In this section, we provide a brief overview of the specific computational methods that form the core of the studies discussed in this review, rather than an exhaustive description of all available ligand- and structure-based computational techniques. To further deepen the knowledge of the different techniques, the reader is referred to the reported literature.

Quantitative Structure–Activity Relationship. Most drugs exert their effects through specific interactions with target macromolecules such as proteins. The interaction involves an interface area where the drug binds the biomacromolecule, and key structural features, namely pharmacophores, are responsible for the biological activity. Quantitative structure–activity relationship (QSAR) modeling aids in designing new active molecules or screening compound libraries, using mathematical models to correlate structural features with biological activity, thus guiding prediction and optimization of drug candidates. The performance of a QSAR model can be estimated using two main coefficients: R^2 (coefficient of determination) measures how well a model fits the training data by quantifying the proportion of variance in observed data explained by the model, values closer to 1 indicate a better fit. Q^2 is similar but assesses the model's predictive ability, typically calculated via cross-validation (such as Leave-One-Out), indicating how well the model can predict unseen data. A high R^2 means good fit to known data, while a high Q^2 means strong predictive power on new compounds. For further reading see Ref. [55].

Homology Modeling. Homology modeling is a computational method for predicting the 3D structure of a protein based on its aminoacid

sequence similarity to one or more known structures (known as templates). If a protein shares a high sequence identity with another protein whose structure is already determined (typically via X-ray crystallography or cryo-electron microscopy), it can be modeled by aligning the sequences and building a structure that mirrors the template folding. The basic assumption of this computational framework is that similar sequences adopt similar structures. In recent years, the field of protein structure prediction has seen a tremendous development thanks to the application of artificial intelligence-based algorithms. For a comprehensive review see Ref. [56].

Molecular Docking. Molecular docking is a computational technique used to predict how a small molecule (referred to as the ligand) binds to a target macromolecule, such as a protein (denoted as the receptor). The technique is widely used in virtual screening of large compounds libraries (up to billions) and has proven to be helpful in the design of new therapeutic compounds. The goal of this approach is to identify the preferred orientation and position of the ligand within the binding site of the target receptor, primarily based on shape complementarity and ligand–receptor interactions, such as hydrogen bonding, hydrophobic contacts, and electrostatic forces. Docking programs also provide a rough estimation of the strength of the binding through so-called scoring functions, that can be physically based or rooted on machine-learning. For further information see Ref. [57].

Molecular Dynamics Simulations. Molecular dynamics (MD) simulation is a computational method used to model the dynamic behavior of biomolecules like proteins, nucleic acids, and membranes over time. By applying the laws of classical mechanics, MD simulates how particles interact and evolve under defined physical conditions such as temperature and pressure. This approach reveals physical insights into structural changes, stability, interactions, and functional mechanisms of biomolecules at the atomistic level. Typical analyses of the MD trajectories include: root-mean square deviation (RMSD), root-mean-square fluctuations (RMSF), radius of gyration that account for system stability and flexibility, and solvent-accessible surface areas (SASA) accounting for the role of solvent molecules. Enhanced sampling MD simulations refer to a set of advanced computational techniques designed to overcome the limitations of conventional MD simulations, which may struggle to capture rare events or transitions due to high energy barriers or slow dynamics. These methods, such as metadynamics, accelerated MD, Gaussian accelerated MD (GaMD), and umbrella sampling, artificially modify the energy landscape or apply biasing forces to increase the probability of observing important conformational changes. This can be done by defining one or more collective variables, which are simplified coordinates that represent the slow, essential motions driving a process in enhanced MD simulations. They compress the complex and high-dimensional atomic motions into a small set of meaningful degrees of freedom that distinguish states or metastable regions. These variables are biased or restrained by techniques like metadynamics or umbrella sampling to accelerate sampling along the relevant transition paths, enabling faster exploration of free-energy landscapes and clearer identification of transition mechanisms. The GaMD, for example, improves sampling and free energy calculations by smoothing the energy surface with a Gaussian-shaped boost potential, which lowers energy barriers and speeds up molecular transitions. It avoids the need for predefined collective variables and allows accurate recovery of the original energy landscape. Enhanced sampling enables more efficient exploration of the system phase space and provides reliable estimates of thermodynamic and kinetic properties, making it particularly useful for studying protein folding, ligand binding, and other complex biomolecular processes. For an overview on MD simulations see Ref. [58].

Free Energy Calculations. Free energy methods are a set of computational techniques used to estimate the thermodynamic stability and binding affinity of interacting molecular systems, such as protein–ligand or protein–protein interactions. These methods quantify the difference in free energy between different states (such as bound and unbound forms), providing insights into how favorable a molecular interaction or conformational change is for the overall stability of the complex. Methods like thermodynamic integration, free energy perturbation, and MM-Poisson/Generalized-Boltzmann Surface Area (MM-P/GBSA), coupled to enhanced sampling techniques, are commonly used. For more reading on free energy calculations see Ref. [59].

3. Receptors

Receptors are crucial targets for drug design, able to trigger an intracellular signal cascade upon binding with a ligand. As a consequence, these proteins play a key role in regulating cellular homeostasis, and their dysregulation can lead to pathological phenotypes, such as cancer. Approximately 35% of approved and marketed drugs target G-protein coupled receptors (GPCRs) [60–62], since they are involved in various relevant physiological processes [63] (Fig. 2). This class of receptors can be modulated through different types of ligands that can enhance, block or decrease their biological activity (*i.e.*, agonists, antagonists, reverse agonists). Generally, regardless of the class of the receptor, its proper regulation leads to a fine-tuning of cellular functions.

3.1. Somatostatin receptor 2

Somatostatin is a 14-amino acid cyclic hormone, that inhibits the release of other hormones like insulin, growth hormone, and secretin by acting as an agonist of somatostatin receptors (SSTRs). These receptors belong to the class A GPCR family and are coupled with inhibitory G-proteins. Among the five SSTR isoforms (SSTR1-5), SSTR2 is the most overexpressed in human neuroendocrine tumors [65]. This makes SSTR2 a significant target for theranostics. Drugs targeting SSTR2 are designed to mimic the structure of somatostatin (both using peptide and non-peptide biovectors). Their development remains a priority due to the great therapeutic and diagnostic relevance of SSTR2 in neuroendocrine tumors [66,67].

In a 2014 study, Cai et al. [22] used a homology model of SSTR2 (the first experimental structures were released later [65]) and molecular docking studies using the Tripos Surflex program [68] to design two new conjugated peptides: CB-TE1A1P–DBCO–Y3-TATE and CB-TE1K1P–PEG4–DBCO–Y3-TATE (where CB-TE1A1P and CB-TE1K1P are cross-bridged cyclam chelators, DBCO and PEG4–DBCO are the linkers, and Y3-TATE denotes the peptide Tyr^3-octreotide [69]). In detail, the authors used four known crystal structures of opioid receptors: the nociceptin/orphanin FQ receptor (PDB ID 4EA3 [70]), the μ-opioid receptor (PDB ID 4DKL [71]), the κ-opioid receptor (PDB ID 4DJH [72]), and the δ-opioid receptor (PDB ID 4EJ4 [73]), with sequence similarities to SSTR2 ranging from approximately 40% to 44%. The alignments were carried out using SYBYL-X 1.3 (Tripos Inc., St. Louis, MO), giving special attention to conserved motifs within the transmembrane regions and to the disulfide bond between Cys115 and Cys193. Manual adjustments were made to improve the alignment of the extracellular loop 2, ensuring that key residues like Pro5.50 and specific motifs such as "D/ERY" in helix 3, "CWFPV" in helix 6, and "NPxxY" in helix 7 were properly aligned with the template structures. The homology model was constructed using Modeler [74] and optimized through an energy minimization. The authors identified the primary binding pocket of the peptides (*i.e.*, near residues Asn276 and Phe294) through site-directed mutagenesis and molecular surface analysis using the visualization program MOLCAD [75], that made possible to detect solvent-accessible cavities surrounding the aforementioned critical residues. Molecular docking studies were then conducted using the Tripos Surflex-docking program [68], and validated by comparing the docking scores of known SSTR2 ligands with their experimentally determined K_i values. This comparison ensured that the docking model accurately reflected experimental binding affinities. The experimental structures of SSTR2 released subsequently [65] confirmed the main findings of the computational study performed on the homology model.

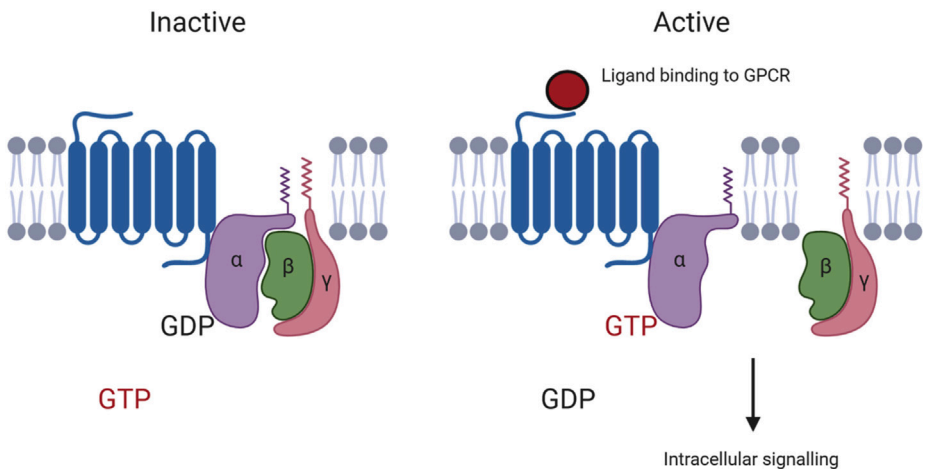

Fig. 2. Agonist induced activation of a GPCR. Class A GPCRs are characterized by a seven-transmembrane helices motif. Upon agonist-mediated activation, these proteins can change conformation and couple with G-proteins at the intracellular side, thus triggering the signal cascade.
Source: Reproduced with permission from Ref. [64].

More recently, Gervasoni et al. used the first experimental structure of SSTR2 to perform an in-depth analysis of the molecular interactions and dynamics features of the receptor with six radiopharmaceutical compounds in clinical use or development (^{64}Cu/^{68}Ga-DOTATATE, ^{68}Ga-DOTATOC, ^{64}Cu-SARTATE, ^{68}Ga-DOTANOC, and ^{64}Cu-TETATATE) [23]. The authors used MD simulations to identify the most stable binding modes and distinct interaction patterns for each compound. In particular, they defined how each component of the radiocompounds (*i.e.*, biovector, chelator, radionuclide) participates in the recognition and interaction with SSTR2. For the parameterization of the chelator–radionuclidde, crucial for the whole study, the authors used the metal center parameter builder (MCPB) module [76] available in the Amber package [77]. MCPB allowed to generate bonded parameters between the coordinating atoms and the radionuclide, using experimental structures of chelators available in the Cambridge Structural Database (CSD) [78] as a reference, and thus avoiding any artifacts due to the non-bonded model [79]. The receptor was embedded into a double layer of phosphatidylcholine (POPC, 70%) and cholesterol (30%) using the CHARMM-GUI server [80]. The system was inserted into a box of OPC water with K+ and Cl– ions. The force field lipid17 was assigned to POPC and cholesterol and ff19SB to the protein. Five replicas of the production runs were carried out for 3 μs, resulting in a total 15 μs simulation time. Interaction patterns between the receptor and ligands were computed using the ProLIF Python library [81]. The substitution of the radionuclide ($^{68}Ga^{3+}$ with $^{64}Cu^{2+}$) was found to have no significant impact on ligand dynamics or key interactions. However, modifications to the chelator moiety (DOTA, TETA, SAR) strongly influenced the interaction pattern. Additionally, subtle structural changes in the peptide at the C-terminal position, and the third residue, significantly altered the dynamics of both the chelator moiety and SSTR2. These findings provided new insights into the molecular basis of SSTR isoform selectivity.

3.2. Cholecystokinin receptor 2

Gastrin and cholecystokinin (CCK), two of the earliest identified gastrointestinal hormones, play critical roles in digestion. They also exert proliferative and anti-apoptotic effects, contributing to carcinogenesis and tumor growth. Elevated expression of gastrin and CCK has been observed in various cancers, including gastric adenocarcinoma, colorectal carcinoma, and pancreatic cancer. The diverse physiological and pathological functions of CCK are mediated primarily by CCK2R, belonging to the class A GPCR family of receptors. The interactions between CCK and its receptor play a significant role in promoting tumorigenesis, making CCK2R a relevant target for cancer therapy [82].

The first experimental structures of the receptor were released in 2021 (PDB ID 7F8W [83]) and 2022 (PDB ID 7XOW [84]). However, in 2018, Lipiński et al. [24] evaluated the binding characteristics to CCK2R of a promising gastrin peptide analog, namely CP04, as well as the impact of different radiometals on this interaction. A binding model of the CP04/CCK2R complex was developed using homology modeling and molecular docking. The structure of CCK2 was generated through homology modeling using the SWISS-MODEL server [85]. The δ-opioid receptor bound to naltrindole (PDB ID 4EJ4 [73]) was automatically selected by the server as the modeling template based on optimal sequence identity, similarity, and coverage. Multiple conformations of the unlabeled CP04 compound were generated and docked in the CCK2R homology model using AutoDock Vina [86]. The docking region was defined as to include the intrahelical cavity, extracellular loops, and surrounding receptor outlet space. The highest-scoring binding poses were then manually reviewed to ensure consistency with existing mutagenesis data on CCK derivatives binding to CCK2R. The authors found that the C-terminal part of CP04 fits into the receptor cavity formed by helices, while the N-terminal, including the DOTA chelator and the metal (Ga^{3+} or Lu^{3+}), is positioned at the binding site outlet, exposed to the solvent. The radiometals influenced only the immediate vicinity of the chelating moiety, leaving the overall conformation unaffected. The predicted model aligns with existing structure–activity relationship data for CCK and CCK2R-targeting radiopharmaceuticals, and it explains the receptor's relative insensitivity to the type of chelated metal, supported by site-directed mutagenesis studies.

3.3. Gastrin releasing peptide receptor

The gastrin-releasing peptide receptor (GRPR), a member of the class A GPCR family, is overexpressed in various malignant tumors across different anatomical sites, including breast, prostate [87], lung [88], and the gastrointestinal tract [89]. GRPR plays a significant role in regulating various human physiological processes, such as gastrointestinal motility, gastric emptying, and smooth muscle contractions. Its endogenous ligand is the gastrin-releasing peptide, which is analogous to bombesin, a 14-amino acid peptide isolated from the skin of the European fire-bellied toad [90]. It is particularly highly expressed in the pancreas, where it induces the release of endogenous gastric hormones and regulates the secretion of pancreatic enzymes [91]. Notably, elevated GRPR expression has been observed in lower-grade prostate

cancer cases, which are typically more challenging to treat. This makes GRPR an important target for diagnostic and therapeutic strategies, offering potential value in the detection and treatment of prostate malignancies [91]. GRPRs have thus gained significant attention in nuclear medicine, particularly as targets for molecular imaging and therapy of prostate and breast cancer.

In this context, Liolios et al. [25] synthesized two bioconjugate probes able to bind GRPR: a bombesin analogue connected to a chelating moiety, with a specific targeting sequence, labeled with ^{68}Ga; and another GRPR-targeting bombesin analogue, incorporating a fluorescent label for easier tracking. The structure of the orexin receptor 2 bound to orexin B (PDB ID 7L1U [92]) was selected as the template for building a GRPR homology model. Using Prime software from Schrödinger [93], homology modeling was performed with an energy-based building approach. The OxB peptide ligand was manually mutated to match the bombesin analogues, including adjustments like linker and chelator additions via Maestro's 3D-build tools. This ensured that the analog retained the backbone orientation of OxB. To understand the interaction mechanisms of the probes with GRPR, the complex was embedded in a hydrated phosphoethanolamine (POPE) membrane bilayer, a 100 ns MD simulation of the membrane-embedded complex was conducted using Desmond with the standard protocol. The authors showed that the probes dived into the GRPR transmembrane helical cavity, where they formed hydrogen bonds and π–π interactions, particularly at the amidated end of the probes. These results provided valuable insights into the molecular interactions of the probes with GRPR, which can be exploited for improving diagnostic imaging and therapeutic strategies involving this target.

3.4. Dopamine receptor

Dopamine is a catecholamine neurotransmitter crucial for neuronal signal transfer and various physiological processes, including reward, addiction, motor coordination, hormonal secretion, glutathione and neuronal energy metabolism. Dysregulation of the dopaminergic system is linked to severe disorders such as schizophrenia, Parkinson's disease, attention deficit hyperactivity disorder, Tourette's syndrome, depression, nausea and vomiting [94]. Advances in gene-cloning techniques have enabled better characterization of the class A GPCR dopamine receptor subtypes (D1–D5). This has facilitated a deeper understanding of their distribution within the central nervous system and their specific roles in various disorders. Such insights are essential for developing targeted therapeutic approaches to modulate dopamine signaling and address these conditions effectively [95]. The D2 dopamine receptor (D2DR) is a critical modulator of dopamine release and a key target for radiopharmaceuticals used in PET imaging. These ligands enable the quantification of dopaminergic pathways in the human brain, and their biophysical characterization provides deeper insights into the mechanisms of their interaction with the receptor.

The work of Moldovean et al. [26] exploited computational techniques to identify different binding patterns of ligands within the same receptor. In detail, the authors used molecular docking, MD simulations, and QM calculations to investigate the interactions between D2DR and three ^{11}C-labeled radiopharmaceutical ligands: raclopride (RACL), FLB457, and SCH23390. These ligands are of particular interest due to their application in PET imaging to quantify dopaminergic pathways. Docking studies carried out on the Swiss Dock server [96] identified two main binding sites for the ligands located at the top and bottom pockets of D2DR. Multiple 50 ns long MD simulations using GROMACS [97] revealed that RACL showed the strongest binding at the receptor's top pocket, consistent with available experimental data. In contrast, FLB457 and SCH23390 exhibited variable binding patterns. RMSF and SASA analyses indicated higher flexibility and solvent exposure for FLB457 compared to the more stable SCH23390. QM:QM' ONIOM [98] calculations with Gaussian [99] was used to optimize the geometry and compute the vibrational frequencies of the complexes. The ωB97XD hybrid exchange–correlation functional was used in conjunction with the 6–311+G(d,p) basis set to expand the molecular orbitals. These high-level calculations confirmed the strong binding affinities of RACL at the top pocket, with high interaction energies correlating with its stability in the binding site. While SCH23390, primarily a D1 receptor antagonist, showed interactions with D2DR, its binding behavior was consistent with lower flexibility. These findings align with previous experimental studies, supporting the use of ^{11}C-RACL and ^{11}C-FLB457 as reliable tracers for imaging D2DR, with new insights into their structural dynamics that enhances the understanding of receptor–ligand interactions.

In silico methods can be used also for exploring the selectivity of compounds towards different isoforms of a protein [67]. The work of Luedtke et al. [27] focused on the synthesis and characterization of compounds with high selectivity for D2 over D3 dopamine receptor subtypes. Previously, substituted phenyl-4-hydroxy-1-piperidyl indole analogues were reported to exhibit nanomolar affinity for D2 receptors with 10- to 100-fold selectivity compared to D3 receptor [100]. Building on this work, a panel of aripiprazole analogues was evaluated, identifying several compounds with similar D2 and D3 selectivity. Molecular docking techniques were applied to visualize the interaction of these compounds with the D2 and D3 receptor subtypes and the binding preferences. Human D2 and D3 receptor homology models, previously published [101], were used as the basis for these computational studies (multiple experimental structures of both isoforms of the receptor have been released later, *e.g.* [102–105]). Docking calculations were performed using the program GOLD [106], with all protein residues treated as rigid to maintain structural consistency during the simulations. A key constraint was introduced, namely a hydrogen bond interaction between the highly conserved transmembrane helix III aspartate carbonyl group and the protonated amine group of the ligand. This interaction forms a conserved salt bridge, critical to ligand binding in both D2 and D3 receptors. These computational docking studies aimed to identify the molecular determinants that confer D2/D3 receptor subtype selectivity, providing insights that could guide the design of future selective D2 receptor ligands for pharmacological and research applications.

3.5. Chemokine receptor 4

The chemokine receptor 4 (CXCR4) belongs to the class A GPCR family and plays a central role in critical cellular processes, including organogenesis, hematopoiesis, inflammation, and immune response, via its interaction with the natural ligand CXCL12. This signaling pathway is implicated in numerous severe diseases such as cancer, HIV, and autoimmune conditions, making CXCR4 a highly attractive therapeutic and diagnostic target [107].

Demmer et al. [28] developed high-affinity CXCR4-targeted peptide ligands for molecular imaging and therapy, leveraging the theranostic potential of CXCR4. The authors introduced the chelator DOTA in ligand design, enabling the incorporation of a wide variety of medically relevant metal ions for imaging and therapeutic applications. Since ligand functionalization can reduce binding affinity, the concept of dimerization, or multimerization, (*i.e.*, including two or multiple biovector portions within one ligand alone [108]) was applied to counteract this effect and maintain high affinity for CXCR4. Starting from an acetylated monomeric CXCR4 antagonist, a series of peptide dimers were synthesized by optimizing the distance between the monomeric units, leading to a 30-fold increase in binding affinity. Molecular modeling studies were conducted to elucidate the binding mode of the dimeric compounds. Given that CXCR4 was crystallized in a dimeric form (PDB ID 3OE0 [109]) in complex with the 18-amino-acid-long peptide polyphemusin, the authors initially explored whether the dimeric compounds could simultaneously occupy both binding sites within the receptor dimer. However, this hypothesis was quickly ruled out due to the significant distance between the two sites (~ 40 Å)

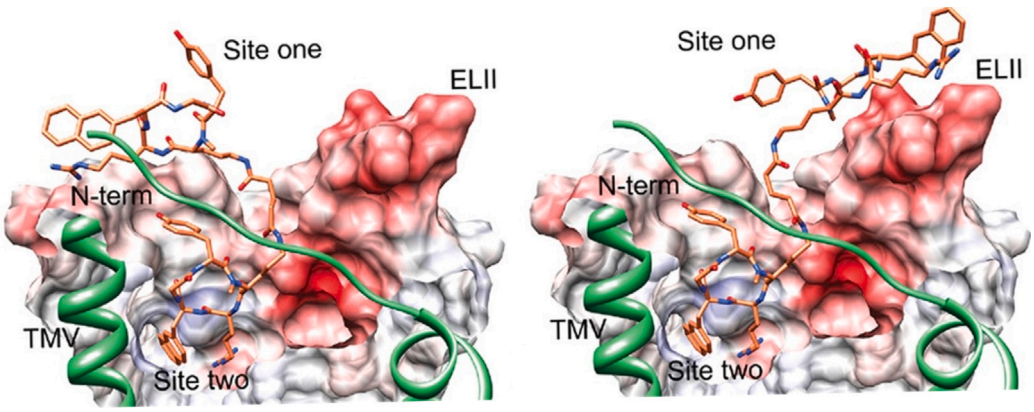

Fig. 3. Alternative binding conformations in the CXCR4 binding site (site one and two). The ligand is represented as orange sticks, while CXCR4 as light-green ribbons and a surface are colored according to its electrostatic potential from red (negative) to blue (positive). ELII: extracellular loop 2, TMV: transmembrane helix 5. (For interpretation of the references to color in this figure legend, the reader is referred to the web version of this article.)
Source: Adapted with permission from Ref. [28].

which exceeds even the longest linker used in their compounds. This finding suggests that the enhanced affinity is likely due to a subsite interaction of the second peptide unit near the main binding pocket. Docking calculations (using Glide [110]) for the dimeric ligands (11 residues with a 5-carbon atom spacer) were considered highly error-prone due to the extreme flexibility of the compounds. To overcome these challenges, the authors adopted a modeling strategy based on the assumption that both ligand monomers would bind the binding site (one in each protein monomer) in the same manner. The dimeric compounds were constructed by integrating the docking pose of one monomer (cyclopentapeptide) of the ligand within CXCR4, with the corresponding linker and the second cyclopentapeptide. Ligand conformations were generated using Glide by identifying several low-energy poses, which were then refined through a Monte Carlo search of nearby torsional minima. This refinement helped optimize the orientation of peripheral groups and, in some cases, adjusted internal torsion angles. These calculations yielded two primary conformational families, wherein the peptide occupying site one either pointed toward extracellular loop II, transmembrane helix II and III, or alternatively, IV and V. The inherent flexibility of site one suggests that this receptor region can adapt dynamically to different dimeric cyclopentapeptides, depending on linker length. The best binding pose closely resembled the experimental binding mode of polyphemusin (Fig. 3).

The concept of polyvalency, and herein more specifically dimers, is particularly interesting in the case of CXCR4 due to the peculiar structure of the receptor which was first hypothesized to contain two neighboring binding sites, one responsible for the affinity and the other for signaling function (“two-site model”) [111]. Furthermore, it is well-known that CXCR4 can form homo- and heterodimers, and this has to be considered as an alternative explanation why some symmetric dimers have superior binding properties as compared to their monomers [112]. However, the spacing of the ligand-binding sites in the crystal structure of dimeric β2-adrenergic receptor matches the ~ 40 Å distance, and this was demonstrated to be approximately the same in the CXCR4 dimers [109]. This suggests that the formation of a functional 2:2 receptor–ligand complex might be plausible for compounds having long linker, while for smaller ligands the same is impossible and the “two-site model” of the receptor seems to be the most reliable hypothesis.

The peptide fragment EPI-X4, derived from human serum albumin and known to inhibit CXCR4, was explored as a scaffold for developing CXCR4-targeting radio-theranostics by Gaonkar and co-workers [29]. The truncated version (JM#21) was conjugated with DOTA to enable radiolabeling with therapeutic and diagnostic radionuclides. Derivatives of JM#21 were synthesized and seven ligands were selected for radiolabeling. To investigate the effect of the ^{177}Lu-DOTA moiety on the binding to CXCR4 of the most promising derivative (JM#173), molecular modeling and optimization were performed using the JM#173-CXCR4 complex structure as a reference. The JM#173-CXCR4 complex (peptide without DOTA) was previously modeled using molecular docking with HADDOCK [113] with the Peptide protocol set, followed by GaMD simulations using NAMD [114,115]. A C-terminal amidated Lys residue with ^{177}Lu-DOTA was attached via an amide bond to the Nϵ atom of Lys6 in JM#173. DOTA coordinates, extracted from the PDB ID 1NC4 [116], were modified by replacing Gd with Lu. The resulting ^{177}Lu-DOTA-JM#173-CXCR4 model underwent docking and optimization to refine the interactions and assess structural compatibility. The C-terminal Lys residue acts as a spacer, positioning the DOTA group in a solvent-exposed region, avoiding steric clashes with CXCR4. The presence of ^{177}Lu-DOTA does not disrupt the peptide’s interaction with CXCR4, and retains the interaction patterns observed in the JM#173-CXCR4 complex.

3.6. Neurokinin-1 receptor

Glioblastoma (GBM), classified as a grade IV glioma by the World Health Organization, is one of the most common and aggressive primary malignant brain tumors. Its prognosis is exceptionally poor, with the majority of patients dying within a year and a median survival time of less than 16 months [117]. Standard treatments, including surgical resection followed by radiotherapy and chemotherapy, have limited effectiveness, as almost all cases experience rapid recurrence. Challenges in treating GBM arise from its heterogeneity, high proliferation rate, infiltrative nature, resistance to systemic drugs, and the restricted delivery of therapeutics due to the blood–brain barrier [118]. A promising experimental approach for enhancing GBM treatment is locoregionally administered targeted radionuclide therapy (TRT). Locoregional administration allows bypassing the blood–brain barrier and minimizes damage to radiation-sensitive organs, while effective diffusion of radioconjugates into the tumor and infiltrative zones maximizes therapeutic efficacy. The neurokinin-1 receptor (NK1R), belonging to the class A GPCR family, is a particularly attractive molecular target for GBM-directed TRT, as it is widely overexpressed in GBM and other gliomas while being minimally expressed in normal central nervous system tissue [119]. Clinical evaluations of locally administered NK1R-targeting radioconjugates have shown promising therapeutic outcomes with minimal toxicity. These studies primarily used peptide vectors derived from the endogenous NK1R ligand, Substance P, or its analogues modified for improved stability. Such peptides have been conjugated with chelators like DOTA or DOTAGA and labeled with radionuclides such

as ^{90}Y, ^{177}Lu, ^{213}Bi, or ^{225}Ac [120]. Despite initial successes, further optimization is needed to enhance the performance of NK1R-directed TRT.

A promising NK1R antagonist, L732,138, has been explored as a radiopharmaceutical vector [121]. This compound exhibits high affinity for NK1R and features a simple structure conducive to SAR studies. Its simplicity allows for the rapid and cost-effective generation of analogues for further evaluation. Matalińska et al. [30] designed and synthesized several novel analogues of L732,138 to investigate whether expanding its structure with potential linking elements would preserve NK1R affinity. In designing bifunctional conjugates, a key challenge lies in determining how and where to attach the typically bulky chelating moiety to the vector fragment without compromising receptor affinity. Therefore, multiple linker lengths were tested to explore different depths of chelator placement within the binding site, including the possibility of directly attaching the chelator. This was done considering the influence of spacers on the lipophilicity of the resulting compounds, modeled experimentally determining the lipophilicity parameter, LogP (octanol–water partition coefficient). Lipophilicity is a critical factor in pharmacology, as it affects a compound's ability to distribute within and accumulate in biological systems. Based on these considerations, the authors designed and synthesized five series of compounds incorporating linkers of various lengths. This strategy allowed the authors to systematically investigate whether introducing potential linking fragments would preserve NK1R affinity. Molecular docking and MD simulations were conducted to understand the SAR of L732,138 and its analogues. Docking was performed using AutoDock [122], with the parent compound optimized at the B3LYP/6-31G(d,p) level in Gaussian09 [99]. Docking was conducted for both *cis* and *trans* conformers of L732,138, and further analogues were manually built from it in the NK1R binding site. Ligand flexibility (except amide bonds) was allowed, while the receptor was treated as rigid. Docking used the experimental structure of NK1R (PDB ID 6HLO [123]), refined via GPCRdb [124] to restore native residues and supplemented side chains. Docking of L732,138 to NK1R revealed that its 3,5-bis(trifluoromethyl)phenyl fragment binds at the bottom of the pocket, engaging in hydrophobic interactions, while the indole ring interacts with transmembrane helices and the N-acetyl fragment is solvent-exposed. No polar interactions were observed, consistent with mutagenesis data showing minimal impact of certain polar residues on binding affinity. Despite initial predictions that directly attaching a bulky chelator (DOTA) to an L732,138 analogue would reduce affinity, experiments showed good binding of the conjugates (*i.e.*, the analogues). Top-scoring docking complexes were embedded in POPC lipid bilayers, solvated with TIP3P water, and ionized. The webserver CHARMM-GUI [80] was used for system preparation with CHARMM36 force fields for proteins, lipids, and TIP3P for water solvent, while ligands were modeled with CHARMM CgenFF. For each system, 3 production runs of 150 ns were performed. Importantly, the chelator was simulated without the radionuclide. MD simulations revealed receptor flexibility, allowing DOTA's integration while maintaining the core structure's deep pocket placement. Minor receptor side-chain adjustments and additional polar interactions with DOTA's carboxylates contributed slightly to binding strength. For longer analogues, docking and MD simulations indicated that the core fragment remains deeply bound, similar to L732,138, while the linker regions exhibit flexibility and form transient interactions with extracellular loop residues. Variations in binding poses and linker rearrangements suggest mobility and adaptability of these longer derivatives, with implications for further SAR studies and optimization of linker designs.

3.7. Metabotropic glutamate receptor

Glutamate is a crucial neurotransmitter in the central nervous system, involved in vital processes such as memory formation, neuronal development, and synaptic plasticity. Glutamate signaling is primarily mediated by two classes of receptors: ionotropic and metabotropic glutamate receptors (mGluRs) [125]. mGluRs are GPCRs that mediate slow and modulatory effects, and they divided into three subgroups based on sequence homology and the signaling mechanisms they trigger: Group I (mGluR1 and mGluR5), Group II (mGluR2 and mGluR3), and Group III (mGluR4, mGluR6, mGluR7, and mGluR8) [126]. The activation of glutamate receptors promotes tumor cell proliferation, metastasis, angiogenesis, and survival by engaging key signaling pathways, and it has been found to be aberrantly overexpressed in various cancer types, including melanoma, breast cancer, pancreatic cancer, and colon cancer.

Xie et al. [31] used ^{211}At-AITM, a small molecule-based radiopharmaceutical that combines tumor-specific targeting of mGluR1 with the potent therapeutic effects of α particle emission. Other pharmacological inhibitors of mGluR1, including riluzole and LY367385, have shown some efficacy in preclinical and early clinical trials. However, their therapeutic potential has been limited by moderate effects and compensatory metabolic mechanisms within tumors [127]. ^{211}At-AITM addresses these limitations by not only causing DNA double-strand breaks but also by downregulating mGluR1 expression and inducing tumor cell senescence. Critical AITM-mGluR1 interactions were revealed by coupling molecular docking and MD simulations. The 3D complex structure of mGluR1-FITM (a known small-molecule antagonist) (PDB ID 4OR2 [128]) was used for molecular simulations. The initial structure of AITM complex was generated using MOE [129]. The FITM and AITM complexes were added within a lipid bilayer and water molecules were placed around the complexes using VMD [130]. For the FITM complex, the energy minimization calculations and 5 ns long MD simulations were performed in the NVT ensemble using Amber18 [77].

The mGluR2 has emerged as a promising therapeutic target for treating various neurological diseases, spurring significant interest in the development of drug candidates that specifically target this isoform. Li et al. [32] synthesized three isoindolone derivatives as novel mGluR2 positive allosteric modulator PET radioligands. Pharmacological evaluations revealed that AZ12559322 exhibited high mGluR2 binding affinity (K_i = 1.37 nM) and displayed excellent selectivity over other mGluR subtypes. The radiosyntheses of [^{11}C]AZ12559322 was successfully achieved with good radiochemical yields, high purity, and high molar activity. To explore the protein–ligand interactions of AZ12559322, it was docked into a mGluR2 homology model. The protein model was constructed using the YASARA software [131], employing template structures from mGluR1 complexed with glutamate (PDB ID 1EWK [132]), mGluR5 complexed with glutamate (PDB ID 3LMK), and the *apo*-form of mGluR5 (PDB ID 6N52 [133]). The models were then used to perform docking studies using AutoDock Vina [86], and the protein–ligand interactions were computed with Schrödinger Maestro. As observed with previous positive allosteric modulators, the binding pocket of AZ12559322 was found to be positioned within the α-helical transmembrane region of mGluR2. The favorable binding orientation was supported by several key interactions. Specifically, AZ12559322 formed a hydrogen bond with the residue Met794 and exhibited π–π interactions with residues Trp643 and Trp773. In the solvent-exposed region, the NH group of the ligand formed a hydrogen bond with the carbonyl oxygen of Met794, with the N–O distance measured at 3.1 Å. Additionally, the indole moiety of the ligand was involved in π–π interactions with two residues, Phe643 and Trp773, with both side chains positioned at a distance of 3.6 Å. This particular binding orientation allowed the indole group to be nestled within a hydrophobic pocket composed of the residues Leu639, Phe643, Leu732, Val736, Ile739, and Val798. These interactions collectively suggest that AZ12559322 could have a high binding affinity for mGluR2, supporting its potential as a strong and effective positive allosteric modulator for this receptor.

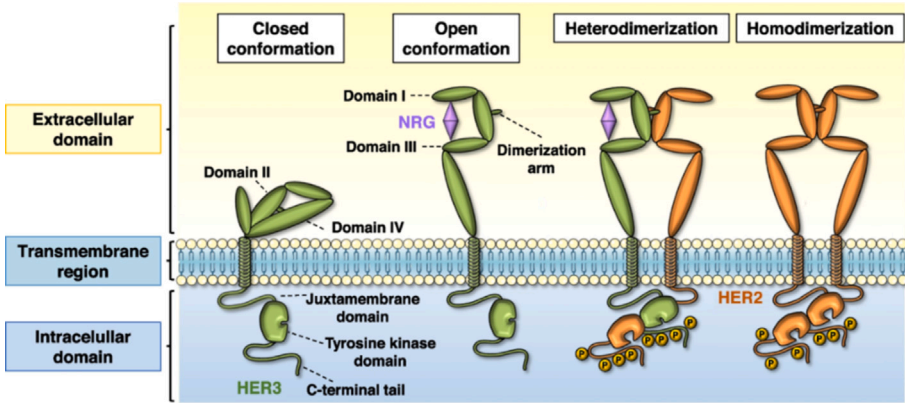

Fig. 4. Schematic representation of the structural changes and activation of HER receptors. Each member is composed of an extracellular region, a transmembrane region, and an intracellular region. The extracellular region is composed of four subdomains (I–IV). When the ligand binds to subdomains I and III, a conformational change is induced in the extracellular domain, leaving the dimerization arm exposed. As a consequence, the receptor can dimerize with another member of the family in open conformation (heterodimerization) or another identical receptor (homodimerization).
Source: Reproduced with permission from Ref. [136].

3.8. Human epidermal growth factor

Human growth factor receptor 2 (HER2) is a member of the epidermal growth factor receptor family. These receptors share a common structural organization consisting of an extracellular domain (ECD), a transmembrane domain, and an intracellular region. The ECD is composed of four subdomains and adopts a closed conformation in the absence of a ligand. Ligand binding induces conformational changes that expose the dimerization arm, leading to receptor homodimerization or heterodimerization, which subsequently activates allosteric kinase signaling pathways and promotes downstream cellular responses (Fig. 4) [134]. HER2 overexpression enhances receptor dimerization, driving uncontrolled cell growth and proliferation. This overexpression is frequently observed in aggressive forms of breast and bladder cancer, where it correlates with poorer patient prognosis and increased tumor progression. Due to its critical role in oncogenesis, HER2 is a key target for therapeutic intervention, with monoclonal antibodies, small-molecule inhibitors, and antibody–drug conjugates being actively used to block its signaling and mitigate tumor growth [135]. For the treatment of HER2 overexpressing cancers, the employment of radiolabeled compounds has played a critical role.

In the work of Sharma et al. [33] molecular docking was used to compare any change in the binding efficiency of the two variants of peptides with good affinity for HER2, using the experimental structure of the HER2 ECD (PDB ID 1N8Z [137]). Peptides were prepared and energy minimized using ACD ChemSketch (ACD/ChemSketch for Academic and Personal Use: ACD/Labs.com, 2018), a 20 Å cube grid box was defined to encompass the active site on the HER2 surface, ten binding poses for each peptide were generated using AutoDock Vina.

In a further study, Binmujlli et al. [34] examined the interactions between radioiodinated compounds such as [^{125}I]anastrozole and [^{125}I]epirubicin and HER2. Notably, they employed molecular docking, MD simulations, and the MM-PBSA method [138]. The results were compared to those obtained for Lapatinib, a known HER2 inhibitor. As part of the study, the authors validated the docking protocol performed with Autodock [122] by redocking TAK-285, the ligand co-crystallized with the HER2 receptor, chosen as the reference structure for the study (PDB ID 3RCD [139]). The docking pose preserved critical interactions between the ligand and the receptor. Moreover, the RMSD between the resolved complex and the one predicted by docking was 1.42 Å, confirming the reliability of the software in reproducing the experimental binding pose. The docking of Lapatinib, [^{125}I]anastronzole, and [^{125}I]epirubicin with the receptor was then used to identify the main interactions involved in the complex binding. For Lapatinib, a docking binding score (ΔG_{bind}) of −10.65 kcal/mol was estimated. It was mainly involved in hydrogen bonds, indicating strong electrostatic interactions contributing to the stability of the binding. [^{125}I]anastronzole, instead, had a slightly higher ΔG_{bind} of −9.65 kcal/mol, and its binding with the receptor was characterized mostly by a network of nonpolar interactions. [^{125}I]epirubicin showed the best binding affinity (ΔG_{bind} = −10.92 kcal/mol) with an average distance of 2.16 Å for the hydrogen bonds network, suggesting highly specific binding. Compared to TAK-285, the radioiodinated molecules formed more hydrogen bonds. Specifically, [^{125}I]epirubicin resulted in a binding mode that could indicate more stable interactions. On the other hand, the interaction pattern of [^{125}I]anastronzole may affect its pharmacokinetic properties. Then, through 200 ns MD simulations done with GROMACS, the author compared again TAK-285, Lapatinib, [^{125}I]anastronzole, and [^{125}I]epirubicin, evaluating the RMSD of both the ligands and the receptor backbone, RMSF, radius of gyration, and MM-PBSA. The HER2 protein backbone showed an average RMSD around 4.00 Å, with the radioiodinated compounds having slightly higher values of 4.35 Å and 4.52 Å for [^{125}I]anastronzole and [^{125}I]epirubicin, respectively. However, even if the RMSD of the ligands is comparable and within what can be considered statistical fluctuations, peaks in the RMSDs of [^{125}I]anastronzole and [^{125}I]epirubicin indicate transient conformational shifts that could play a role in their mechanism of action. The RMSF of all the complexes did not deviate from the flexibility pattern expected for HER2. Nonetheless, the radioiodinated molecules reached peaks of about 6.1 Å for the residues 47 to 67 and 125 to 135, possibly revealing areas of the protein where allosteric effects or changes in protein dynamics might alter their binding ability. The greater flexibility of the receptor in complex with these ligands was also demonstrated by the radius of gyration, which exhibited a broader range of values compared to the other compounds studied. To provide a quantitative measure of interaction strength and stability, the authors evaluated the hydrogen bond profile from the MD simulations. Interestingly, [^{125}I]anastronzole presented an average of two persistent hydrogen bonds, the same as TAK-285. [^{125}I]epirubicin, however, exhibited four hydrogen bonds — the highest number — considering that Lapatinib had an average of three. Having a high number of hydrogen bonds suggested stronger interaction with the receptor and probably a higher binding affinity. To complement these insights, the authors executed MM-PBSA calculations using g_mmpbsa, a GROMACS software suite component, to estimate the binding free energy of the different ligands [140]. Consistently, [^{125}I]epirubicin showed the most favorable binding energy, equal to −68.81 ± 0.12 kJ/mol, with the electrostatic component (−37.44 ± 0.17 kJ/mol) surpassing those of Lapatinib and

TAK-285. [^{125}I]anastronzole, despite showing a higher binding free energy compared to TAK-285, has smaller affinity than Lapatinib. Overall, this study elucidated important details on the interactions and stability of different complexes involving HER2, offering promising expectations for the studied radioiodinated molecules.

3.9. αβ integrins

Integrins are essential cell adhesion receptors that function as linkers between cells and the extracellular matrix (ECM), acting as bidirectional hubs for transmitting biochemical and mechanical signals. Among them, integrin $\alpha v\beta 3$ is a key family member that interacts with ECM proteins containing the tripeptide sequence RGD (Arg-Gly-Asp). This family consists of two non-covalently bound type I transmembrane glycoprotein αv subunits and $\beta 3$ subunits, both of which consist of a large extracellular domain, a single transmembrane helix and a short cytoplasmic structure domain. Increasing evidence has shown that abnormal overexpression of $\alpha v\beta 3$ is implicated in multiple aspects of tumor progression, including tumor initiation, sustained growth, metastasis, drug resistance, and the maintenance of cancer stemness. Due to its significant role in cancer biology, $\alpha v\beta 3$ integrin has been extensively explored as a therapeutic target across various cancer types. However, despite considerable efforts, to date no $\alpha v\beta 3$ antagonist has been approved for clinical use [141].

Pirooznia et al. [35] investigated a ^{68}Ga-labeled cyclic RGD peptide designed to target $\alpha V\beta 3$ integrin. RGD peptides have the ability to act as diagnostic probes for the early detection of growing tumors. The authors redocked various RGD-containing peptides into the crystal structure of $\alpha v\beta 3$ (PDB ID 1L5G [142]) using the HADDOCK webserver [113], defining Asp150, Asp218, and Arg216 as the active site residues. HADDOCK incorporates experimental or predicted interface data as interaction restraints to guide docking, it is capable of modeling complexes involving proteins, nucleic acids, and ligands. The top 10 docking poses were then subjected to 20 ns of MD simulations using GROMACS with the CHARMM36 force field. The stability of all simulations was assessed through several metrics, including RMSD, radius of gyration, temperature, density, and pressure fluctuations. Finally, an MM-PBSA calculation was performed to estimate the total energy and binding affinity. Based on their analysis, the authors confirmed that all selected structures were stable. The one with the lowest energy (−2308.72 KJ/mol) was selected for further experimental studies.

Integrin-$\alpha 6$ is another attractive diagnostic and therapeutic biomarker. Chen et al. [36] designed a cyclic peptide ligand, NOTA-A6P, with enhanced binding affinity towards integrin-$\alpha 6$, that has been labeled with aluminum-[^{18}F]fluoride [143]. [^{18}F]AlF-NOTA-A6P, was subsequently developed for PET imaging to enable the early detection of colorectal cancer. In this work, the authors started from the integrin-$\alpha 6$ targeting peptide (CRWYDENAC), and generated a series of modifications, using alanine scanning, D-substitution, truncation, and dimerization. The resulting peptides included both linear and cyclic (A6P) and linear peptides. To further optimize targeting properties, molecular docking studies were performed using the crystal structure of human integrin-$\alpha 6$ (PDB ID 7CEC [144]). The docking analysis predicted the binding modes and interactions between A6P and integrin-$\alpha 6$, providing the foundation for the design of a novel fluorine-18 radiolabeled peptide, NOTA-A6P. This new compound was synthesized by coupling A6P with a PEG4 spacer and a metal chelating group (NOTA) to facilitate fluorine-18 labeling. To refine structural predictions, the integrin-$\alpha 6$ model was further optimized using SWISS-MODEL homology modeling [85]. The 3D structure of the peptide was generated via the PEPstrMOD server [145], followed by unbiased docking to integrin-$\alpha 6$ using ZDOCK [146]. The MOE software was used to analyze protein-peptide interactions, and the optimal docking mode was selected based on binding strength and interaction sites. These computational insights guided the rational design of NOTA-A6P, leading to improved targeting efficiency and stability for PET imaging applications.

3.10. Translocator protein

The translocator protein (TSPO) is a five-transmembrane domain protein that is widely expressed throughout the body. It is predominantly found in steroid-producing tissues, while its expression in the healthy central nervous system is minimal. However, TSPO expression significantly increases in activated glial cells within areas affected by neurodegenerative diseases [147]. This upregulation can be visualized using molecular imaging techniques, such as PET, allowing for the detection of neuroinflammation in both preclinical and clinical studies of neurodegenerative disorders. Additionally, elevated TSPO expression in cancer cells has drawn interest as a potential biomarker for tumor growth and a novel target for chemotherapy [148]. However, clinical utility of second-generation TSPO ligands as biomarkers has been limited due to the rs6971 polymorphism, which significantly affects ligand binding affinity in humans.

Lee et al. [37] used molecular docking to investigate the interaction of a new fluorinated TSPO-ligand (BS224) with the binding sites of rat wild-type and mutated TSPO. Homology models of wild-type and A147T mutant TSPO were generated using mouse TSPO structures as templates, leveraging their high sequence identity (94%). Missing residues were modeled with Prime's energy-based method, retaining the template's ligand (PK11195), an analog of BS224 [149]. The ligand BS224 was prepared with LigPrep to consider tautomers and physiological ionization states. Docking was carried out using Glide in extra precision mode, with full ligand flexibility and partial protein side-chain flexibility (for Thr147 and Thr148). A cubic grid centered on PK11195's position guided docking. BS224 docking was constrained to poses aligning with PK11195's shared substructure within a 2.0 Å RMSD tolerance. The authors found that the binding mode of BS224 was not affected by the mutation and consequently supported the observed *in vitro* selectivity of [^{18}F]BS224 regardless of polymorphisms.

3.11. Challenges for computational studies of receptors

Receptors are typically embedded into a double layer membrane. Therefore, a further challenge related to these systems is to properly model biological membranes in terms of composition and physical behavior. Moreover, the study of interactions between membrane components and the receptors or the radiopharmaceuticals is often neglected, although it can influence the binding activity. Furthermore, several of the studies mentioned in this section used homology modeling to obtain the 3D structure of the receptor. The most conserved portions are usually the transmembrane ones, whereas the most flexible regions exposed to solvent, such as loops, are more variable. For this reason, generally the models of the transmembrane segments are more solid than those of the loops. However, the loops are often the major responsible of specificity and isoform selectivity, therefore extra attention should be paid to their modeling.

4. Enzymes

Several radiopharmaceutical targets are enzymes overexpressed in multiple tumor types. Generally, molecules targeting enzymes are inhibitors that firmly bind the active binding pocket, preventing the catalytic activity of the enzyme and, depending on the radionuclide, possibly functioning as radiotracers. Among the most targeted enzymes there are the prostate-specific membrane antigen and, more recently, the fibroblast activation protein α. However, other enzymes have been targeted over the years, such as the choline kinase (ChoK), the poly-ADP ribose polymerase (PARP) [150], and the acetyl/butyrylcholinesterases (AChE/BuChE) [151].

ChoK, overexpressed in many tumors, catalyzes the conversion of choline to phosphocholine, leading to the trapping of phosphocholine in cells. This whole metabolic process forms the basis for investigation of choline analogues as radioprobes for tumor imaging. The structural

properties and steric hindrances introduced into the choline backbone by the incorporation of ^{18}F have been extensively studied. Jaswal et al. [152] performed molecular docking using AutoDock Vina and the crystal structure of ChoK in complex with phosphocholine (PDB ID 2CKQ [153]). Modeling of the ligand was carried out using ChemDraw (Revvity Signals Software, Inc.), and its energy-minimized 3D coordinates were generated with OpenBabel [154]. Results were analyzed using BIOVIA Discovery Studio visualizer (BIOVIA, Dassault Systèmes, San Diego: Dassault Systèmes) and showed that two of the methyl groups play a crucial role in maintaining the molecule's affinity for ChoK. Whereas, the third methyl group can be modified or replaced by an alkyl chain, which can be linked to a radionuclide.

Most ^{18}F-labeled PARP inhibitors are structurally related to Olaparib (a known PARP inhibitor), however since their hydrophobic properties, they are mainly excreted by the liver and bile, resulting in a high accumulation of radioactivity in the abdomen. Wang et al. [155] used molecular docking to evaluate whether the introduction of a DOTA moiety could fit within the binding pocket. AutoDock Vina was used to dock the ligands into the experimental structure of PARP in complex with Olaparib (PDB ID 5DS3 [156]). They found that ^{68}Ga-labeled radiotracers based on Olaparib can be a promising alternative for monitoring ovarian cancer tissues with elevated PARP expression and detecting abdominal tumor metastases.

AChE and BuChE are responsible for the degradation of neurotransmitter acetylcholine [151]. This mechanism leads to age-related brain disorders, such as Alzheimer's disease (AD). Tacrine, a cholinesterase inhibitor, is the first drug approved by the Food and Drug Administration for palliative treatment of AD, but its usage is limited by significant development of hepatotoxicity and cardiovascular system impairment, while not having significant cognitive effects [157]. However, due to its biological activity towards AChE and BuChE, radiopharmaceuticals based on tacrine, coupled to diagnostic radionuclides, can be used for the imaging of regions with high concentrations of cholinesterases [158]. In a study aiming to synthesize and investigate recently designed radiolabelled analogues of tacrine [^{99m}Tc]Tc-Hynic-(tricine)2NH(CH2)ntacrine ([^{99m}Tc]Tc-Hynic-NH(CH2)nTac) and ^{68}Ga, [^{68}Ga]Ga-DOTA-NH(CH2)ntacrine ([^{68}Ga]Ga-DOTA-NH(CH2)nTac), Gniazdowska et al. [159] used molecular docking on the two most promising radioconjugates, [^{99m}Tc]Tc-Hynic-NH(CH2)9Tac and [^{68}Ga]Ga-DOTA-NH(CH2)9Tac. 3D structures of the compounds were drawn in Maestro and geometry-optimized using Density Functional Theory (DFT)-B3LYP with the LACV3P** basis set in Jaguar [160]. Crystal structures of AChE in complex with donepezil (PDB ID 4EY7 [161]) and BuChE in complex with butyrate (PDB ID 1P0I [162]) were used for docking. The protein structures were prepped in Hermes (CSD-Core Suite, Cambridge Crystallographic Data Centre), and the binding sites were defined as residues within 10 Å of donepezil for AChE and 20 Å of glycerol for BuChE. AChE residues Tyr337 and Trp286 were modeled flexibly to account for possible rotamers. Docking was conducted using GOLD with default genetic algorithm parameters [163]. Results were evaluated via the GoldScore function and visual inspection, generating 10 ranked conformations per ligand. Technetium and gallium, lacking native parameters in GOLD, were modeled using manganese and aluminum ones. The authors compared them with a reference tacrine, highlighting that both compounds interact in a similar way with AChE and BuChE catalytic and peripheral active sites. However, the tacrine portion seemed to be the most important, and assumed the same conformation as in the complexes of tacrine alone with the two cholinesterases (Fig. 5).

4.1. Prostate-specific membrane antigen

Prostate-specific membrane antigen (PSMA) is an enzyme that is primarily expressed in prostate tissue, particularly in prostate cancer cells. It is a type II transmembrane protein with enzymatic activity, functioning as a glutamate carboxypeptidase. PSMA plays a role in breaking down specific molecules in the nervous system and small intestine, but it is most notable for its high expression in prostate cancer, where it is used as a biomarker [164]. Due to its elevated presence in malignant prostate tissues, PSMA is a key target for diagnostic imaging and targeted therapies, including radioligand therapies for prostate cancer [165]. From a computational point of view, the treatment of this enzyme is challenging due to the presence of two catalytic zinc ions in the binding pocket, that participate in the reaction mechanism, and also due to the peculiar shape of the binding pocket which has an elongated and narrow L-shape, and it is constituted by multiple sub-pockets (*i.e.*, P1, P1', arginine patch) (Fig. 6). Therefore, PSMA inhibitors need to fit the pocket conformation and generally interact with the zinc ions to stabilize the binding.

Molecular docking has been applied to test whether radiopharmaceuticals could insert within the binding pocket and how they interact in details with PSMA. Specifically, the most used zinc-binding group is glutamate-urea-based, proposed by Kozikowski and colleagues [167], that mimics the substrate without being metabolized. Then, multiple scaffolds have been proposed to interact with the other parts of the binding pocket. Wang et al. [38] developed ^{123}I-based radiopharmaceuticals using as a first step molecular docking to test the binding of compounds to PSMA, considering the protein as rigid (PDB ID 3D7H [168]) and the ligand as flexible. They used AutoDock Vina with the grid box covering the whole active site and generating 10 poses. Similarly, other two works adopted molecular docking, using other structures of PSMA (PDB ID 2C6C [169] and 5O5T) and settings (Glide and ADFR suite [170], where ions and water molecules in the buried part of the binding pocket were kept) to test the binding of inhibitors into PSMA, also considering the chelator DOTA in complex with either ^{99m}Tc or ^{68}Ga [171,172]. Often these peculiar atoms cannot be handled by docking programs, therefore the user can change the atom type and assign the appropriate charge (*e.g.*, changed the atom type Tc to Mn without affecting any atomic coordinates and assigned a charge of +2 to Mn [171]). Differently, Liolios et al. simulated radiopharmaceutical inhibitors containing the chelators, without the inclusion of the radionuclide [39,173]. In particular, they combined docking with MD simulations to study the interaction and stability of a ligand containing HBED-CC (a common acyclic chelator) and PSMA, showing a crucial hydrogen bond network participated also by the chelator [173]. The structure with PDB ID 3D7H was selected and prepared using the Schrödinger Protein Preparation Wizard, followed by an energy minimization performed with the OPLS2005 force field. The top-scoring docking pose of the ligand was placed in a TIP3P water box with 0.150 M NaCl. A 100 ns MD simulation was run using Desmond (Schrödinger, New York, NY, 2025), following the default protocol for soluble proteins.

4.2. Fibroblast activation protein α

Fibroblast activation protein α (FAP) is a transmembrane serine peptidase, presenting a catalytic triad made by a catalytic serine (Ser624) and a histidine (His734) and aspartate (Asp702). It is overexpressed in most epithelial cancers by stromal fibroblasts, that infiltrate almost all solid tumors making this enzyme a pan-tumor marker, with minimal expression in healthy tissues [174]. Since in cancerous tissues its expression is linked to tumor invasiveness, metastatic potential, and poor prognosis [175], great efforts have been put into the discovery and design of compounds able to inhibit FAP activity. Different small molecules have been designed to target and inhibit FAP, which are mostly covalent inhibitors attacking Ser624, based either on boroPro (mimicking the catalytic reaction transition state) or cyanopyrrolidine analogues [176]. These scaffolds have been also conjugated with chelators carrying radionuclides. Only a few computational studies based on molecular docking have been performed on this target [177–179], some of which focusing only on the precursor scaffold of the radiodrug [180,181], while others considered also the chelator moiety. The

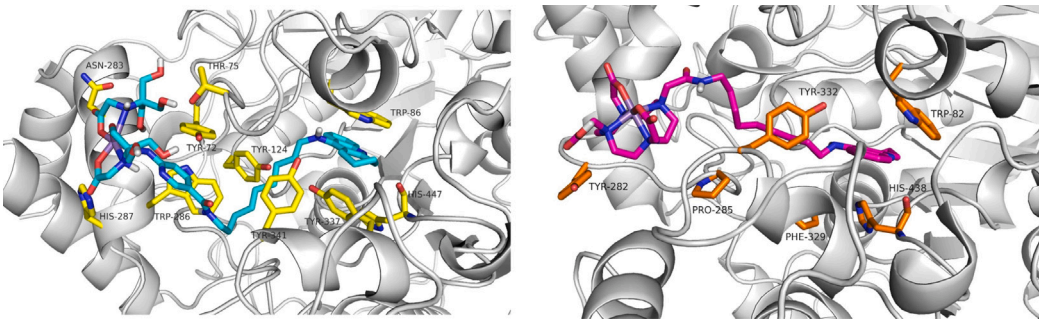

Fig. 5. Left: binding mode for compound [^{99m}Tc]Tc-Hynic-NH(CH2)9Tac (cyan sticks) within the active site of AChE (white cartoon and yellow sticks). Right: binding mode for compound [^{68}Ga]Ga-DOTA-NH(CH2)9Tac (magenta sticks) within the active site of BuChE (white cartoon and orange sticks).
Source: Reproduced with permission from Ref. [159].

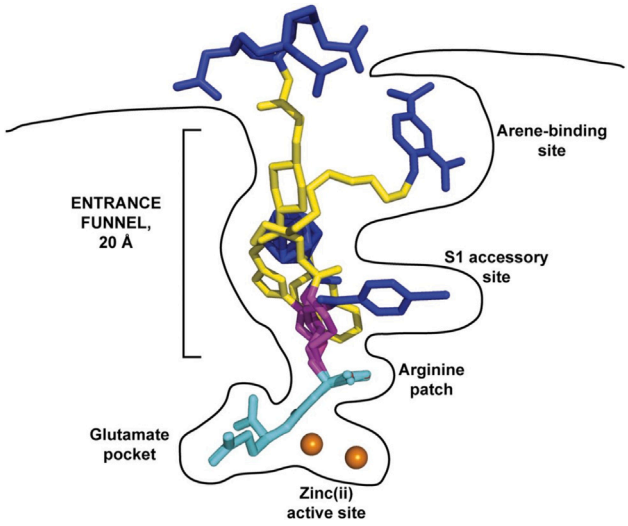

Fig. 6. Binding cavity of PSMA. All sub-pockets of PSMA are reported with glutamate-urea–based ligands (colored sticks). Zinc ions are shown as orange spheres. (For interpretation of the references to color in this figure legend, the reader is referred to the web version of this article.)
Source: Reproduced with permission from Ref. [166].

inclusion of this portion in the docking calculation can be treated considering the coordination geometry of the chelator (when in complex with a radionuclide) [41,182], or keeping the chelator portion flexible and free to assume any conformation [183,184]. In the latter case, the docking software would try to enhance the contacts and interactions between the ligand and the protein, by using also functional groups that should be involved in the radionuclide chelation. Therefore, the user should pay extra attention to the results and consider that the whole radiopharmaceutical could behave differently. Generally, it is safer to simulate the chelator in the right coordination geometry, depending on the radionuclide that will be loaded. In a recent study of Galbiati et al. [40] the crystal structure of DOTAGA in complex with ^{68}Ga was downloaded from the CSD and used to generate the starting conformation of the ligands, and the chelator portion was maintained fixed during docking calculations, performed using the GOLD software [163]. All the monomers of the two available experimental structures of FAP were used to perform ensemble docking, in order to indirectly consider the binding pocket flexibility. Two scoring functions were used (ASP and PLP), the ligands were treated as flexible, and the docking region was defined as a 20 Å sphere centered on Ser624. For each docking run, 100 poses were generated, obtaining overall 1200 poses per ligand (six pockets, two scoring functions, 100 poses each). The best poses were selected based on the docking score and the orientation of the cyanopyrrolidine moiety within the binding site. All compounds exhibited a common binding mode within the catalytic site, where the cyanopyrrolidine headgroup interacted with Ser624 and adjacent residues. The binding pocket contained three potential sub-sites (SITE A–C) for the DOTAGA payload, each contributing to the stabilization of the FAP–ligand interaction. Two of these sub-sites (SITE A and SITE B) were located inside the binding pocket, whereas SITE C was positioned externally. Bulkier FAP derivatives predominantly occupied SITE C, while smaller ligands tended to engage SITE A and SITE B, or regions between them. Another strategy has been used by Li et al. [41] where covalent docking was applied, using CovDock [185] workflow in the software package of Schroödinger in which non-covalent docking is followed heuristic identification of the covalent attachment site, and structural refinement of the resulting complex. A recent study [42] designed and optimized FAP-targeting radiopharmaceuticals by developing QSAR models. In detail, the authors collected a dataset of 36 FAP inhibitors, for which several molecular descriptors were computed. First, stepwise regression and genetic algorithms were used to construct predictive 2D-QSAR models via multi-linear regression, obtaining high coefficients of determination and cross-validated accuracy. Then, to capture spatial and physicochemical features relevant to molecular recognition, 3D-QSAR models were generated using comparative molecular field analysis (CoMFA) and comparative molecular similarity indices analysis (CoMSIA). The CoMFA model showed superior predictive metrics, highlighting steric effects as major contributors to activity, while CoMSIA revealed that hydrophobicity and hydrogen bonding also play key roles. The models were further validated with external datasets, including radiopharmaceuticals in clinical or preclinical stages and small molecule FAP inhibitors, with consistent prediction accuracy. Important molecular descriptors were identified, such as autocorrelations weighted by atomic polarizability, ionization potential, and electronegativity in 2D models, and spatial features relating to steric bulk and hydrophilic/hydrophobic regions around pharmacophores in 3D models. Finally, virtual screening based on these QSAR models identified 23 FDA-approved drugs as promising inhibitors.

4.3. Challenges for computational studies of enzymes

One of the crucial step in modeling drug–enzyme interactions is the correct setup of the binding pocket, especially concerning the ionization states of the catalytic residues. This can be particularly tricky when metal cofactors are present in the pocket, as participants of the catalytic mechanism. In this case, extremely care should be paid to the proper parameterization and modeling of the coordination geometry (see Section 9), that also defines how the drug interacts inside the binding pocket. In this regard, often the solvent (*i.e.*, water molecules or hydroxide ions) can participate the catalytic mechanism. In such a

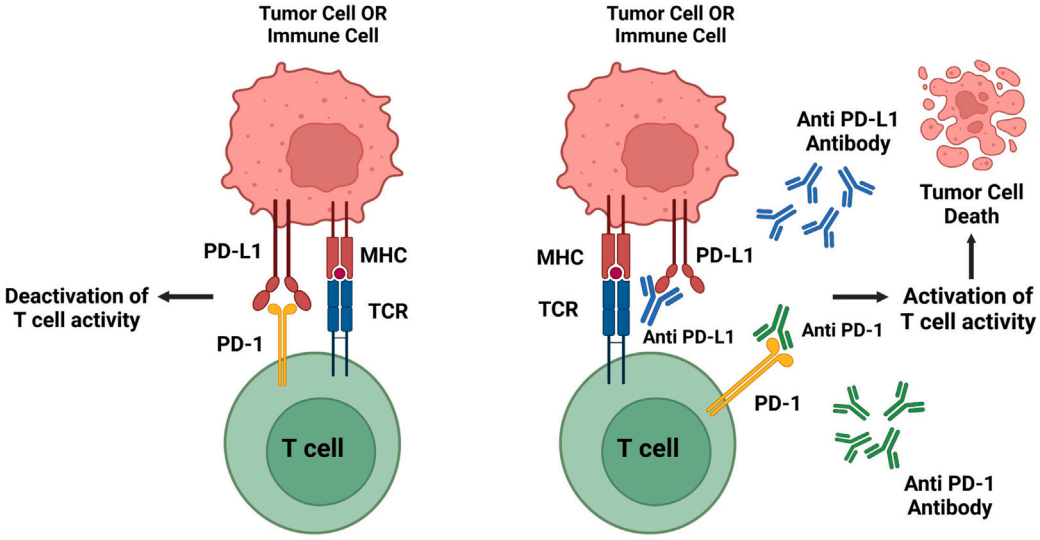

Fig. 7. The interaction between PD-1 expressed by the *T* cell and PD-L1 expressed by the tumor cell deactivates *T* cell activity. When an anti-PD-L1 agent is introduced, PD-1 can bind to anti-PD-1 antibody, leading to activation of *T* cell activity and subsequent tumor cell death.
Source: Reproduced with permission from Ref. [189].

case, it is important to assess whether to include the solvent in the calculation (for instance in docking or QM/MM simulations), as it can radically change the way the drug interacts with the enzyme. Finally, when working with covalent inhibitors, covalent docking can be chosen to model the attach of the inhibitor to the enzyme. However, given the limitation of molecular docking (*e.g.*, limited sampling, rigid protein, basic parameterization), this method should be used only when a suitable enzyme structure is available (no rearrangement of the binding pocket needed), and the whole catalytic mechanism is well known.

5. Immune escape proteins

Immune escape is a key mechanism by which tumor cells evade the host's immune response, allowing them to survive. Programmed cell death protein 1 (PD-1) and its ligand PD-L1 play crucial roles in this process by modulating immune responses. The interaction between PD-1 on tumor-infiltrating lymphocytes and PD-L1 expressed by tumor cells triggers pathways that dampen immune cell activity, notably reducing the proliferation of antigen-specific CD8+ T cells [186]. Blocking the PD-1/PD-L1 axis reactivates *T* cells, enabling them to recognize and attack cancer cells (Fig. 7). Radiation therapy can increase PD-1 and PD-L1 expression, creating an immunosuppressive environment that fosters resistance. Combining radiotherapy with immune checkpoint inhibitors targeting PD-1 [187] or PD-L1 aims to amplify immunogenic effects while reducing immunosuppression [188].

Chatterjee et al. [43] developed a highly potent (IC_{50}= 23 nM) 14-amino acid cyclic peptide, ^{64}Cu-WL12, targeting PD-L1. The authors used molecular docking of WL12 (excluding the chelator NOTA and the radionuclide) to PD-L1 (PDB ID 4ZQK). A conformational search, using the Prime module of the Schrödinger suite, generated 100 peptide conformers, and docking was conducted using Glide. The peptide WL12 was found to form a β-sheet structure within the binding groove, mimicking critical binding interactions of PD-1. Afterwards, different works were published in which molecular docking was used to design new peptides able to inhibit PD-L1, with different features (*e.g.*, PEGylation [44]) and chelator–radionuclide pairs (*e.g.*, ^{68}Ga-DOTA [45], [^{18}F]AlF-NOTA [46]). More recently, Ferro-Flores et al. [47] designed and synthesized a radiolabeled cyclic peptide, [^{99m}Tc]Tc-iPD-L1, targeting PD-L1 for SPECT imaging. The study employed molecular docking using AutoDock Vina to predict and analyze the binding affinity and interaction sites of iPD-L1 and its HYNIC conjugate (that allows the conjugation with the radionuclide [190]) with the PD-L1 receptor. The simulations were performed without including ^{99m}Tc and the chelator in the ligand. Results showed that HYNIC conjugation improved the binding affinity of iPD-L1 by increasing favorable interactions, notably ionic and hydrogen bonds, at key PD-L1 residues, supporting its high specificity. Clinical SPECT/CT imaging in a patient with malignant melanoma demonstrated that [^{99m}Tc]Tc-iPD-L1 can detect PD-L1 positive lesions and differentiate them from PD-L1 negative ones, indicating its potential for patient stratification in immunotherapy. The same authors [48,49] developed two novel radiotracers: [^{18}F]AlF-NOTA-iPD-L1 and ^{177}Lu-DOTA-iPD-L1, both targeting and inhibiting PD-L1. In both cases, molecular docking with AutoDock Vina was used to investigate the interaction of the inhibitor peptides (including the chelators, but not the radionuclide) with the PD-L1 protein. The inhibitor structures were prepared using a pre-optimized geometry generated using the MMFF94 force field, followed by QM semiempirical optimization (using PM7 and PM6 Hamiltonians, respectively) with Mopac2016 [191]. The computational studies supported the design and validation of the novel peptide-based radiotracer by identifying key residues involved in the binding interface and potential conformational stability of the complex.

5.1. Challenges for computational studies of immune escape proteins

When targeting an immune checkpoint regulation protein, the challenges are the same as targeting an epitope: the ligands do not bind to a pocket, but to a surface. This means that the target region is usually broad and very exposed to solvent, that is the definition of a undruggable site. Therefore, for this type of proteins, ligands such as peptides or proteins (*e.g.*, monoclonal antibodies) are more suitable than traditional small molecules. Often, molecular docking is the first choice to model such interaction, however, it should be followed by MD simulations to assess the stability of the complexes and the role of solvent.

6. Transporters

Membrane transporters have a central role in physiological functions as they not only engage the transport of endogenous substrates, but also xenobiotics (including drugs) [192–194].

6.1. Glucose transporters

The characteristics of cancers have been strongly linked to the expression levels of glucose transporters (GLUTs). Overexpression of transporters like GLUT1 and GLUT3 is associated with increased tumor aggressiveness, invasiveness, malignancy, and a higher likelihood of metastasis [195]. The reason behind this strong correlation lies in the metabolic preferences of cancer cells, those exponential growth often induces hypoxia in cells. Under these conditions, cancer cells adopt a unique form of metabolism, where they produce lactate as an end-product of glycolysis rather than fully oxidizing glucose, a process known as the "Warburg effect". Since glycolysis is much less efficient than oxidative phosphorylation, cancer cells require a higher glucose intake compared to normal cells. This increased glucose uptake is facilitated by the upregulation of glucose transporters, particularly GLUT1 and GLUT3, which are responsive to hypoxic conditions. This overexpression of glucose transporters is also leveraged in diagnostic methods such as [^{18}F]fluorodeoxyglucose-PET (FDG), where the high glucose uptake by cancer cells can be visualized [196]. Kilicoglu et al. [197] performed docking studies to examine the mechanism of action of FDG and the effect of its radiation on GLUT1. One challenging task is to correctly represent and simulate the carbohydrate geometries, therefore they used density functional theory level of theory to optimize the FDG geometry. Many breast cancers do not exhibit elevated glucose metabolism, which is primarily facilitated by the GLUT1 transporter, and may instead use fructose as an alternative energy source. The primary transporter for fructose in cancer cells is GLUT5, and elevated levels of this transporter have been observed in human breast cancer. This suggests an alternative approach for early detection using fructose analogs (FDF).

Another challenge when working with GLUTs is the multiple macro-conformations that the transporters can assume, of which not all have been solved experimentally (Fig. 8) [198]. To investigate the specific binding requirements of GLUT5, Rana et al. [50] designed, synthesized, and screened a new class of fructose mimics based on the 2,5-anhydromannitol scaffold. To better understand the interactions between hexoses and GLUTs, the authors minimized the ligand conformations using MMFF94x and LigPrep. Docking was performed using Glide XP with the GLUT5 receptor (PDB ID 4YB9 [199]), generating 10 poses per ligand, with top-scoring ones selected for MD simulations. Systems were embedded in POPC lipid bilayers via CHARMM-GUI, solvated with TIP3P water, and ionized to 0.15 M NaCl. Amber18 was used for setup, applying ff14SB and lipid14 force fields, and ligands were parametrized with Antechamber (GAFF and AM1-BCC charges). MD simulations were run for 50 ns, and MM/GBSA calculations were performed on production snapshots using MMPBSA.py to estimate binding enthalpy. These simulations provided insights into the structural preferences of GLUT5 for certain ligands compared to other glucose transporters, helping guide the design of more selective fructose-based probes for early cancer detection.

6.2. Dopamine active transporter

The dopamine active transporter (DAT) is a member of the solute carrier family 6, that clears dopamine from the synaptic cleft and is central to dopaminergic signaling and many neuropsychiatric disorders. It possess 12 transmembrane helices, and cycles through outward-open, occluded, and inward-open conformations during transport. Different ligands stabilize distinct conformational states, for instance, substrates like dopamine bind to the outward-open form and trigger structural transitions toward occluded and inward-open states to allow substrate translocation. Some ligands such as cocaine analogs stabilize the outward-open state by preventing closing of extracellular gates, while atypical inhibitors like benztropine analogs preferentially bind and stabilize the inward-open or occluded states. This ligand-dependent stabilization affects the dynamics and accessibility of the transporter's binding sites and gates, thereby influencing transport activity and inhibitor potency [201]. PET and SPECT imaging of DAT has been employed to assess the integrity of dopaminergic nerve terminals during normal aging and pathological conditions such as Parkinson's disease, facilitating early diagnosis and monitoring of disease progression and treatment response [202].

In a recent paper, Castillo-Garit et al. [51] presented a combined computational approach integrating QSAR modeling, molecular docking, and MD simulations to aid the design of novel radiotracers targeting DAT for Parkinson's disease diagnosis. The study used a structurally diverse dataset of 57 compounds with known DAT affinity (dissociation constants Kd) to develop a multiple linear regression QSAR model. Molecular descriptors were calculated using Dragon software [203], and the variables were selected via a genetic algorithm within the QSARINS platform [204]. The final QSAR model incorporated four key molecular descriptors and showed good fit and predictivity with R^2=0.755, Q^2=0.680, and external validation R^2_{ext}=0.709. Virtual screening of eleven structurally diverse compounds relevant to the central nervous system was performed with this QSAR model, identifying several molecules with predicted DAT affinity comparable or better than the reference radiotracer ^{123}I-Ioflupane. Molecular docking with Autodock Vina using the human DAT crystal structure (PDB ID 8Y2D, outward-open state of DAT in complex with dopamine) verified docking poses and binding energies consistent with the QSAR affinities. Selected docking complexes underwent 100 ns MD simulations demonstrating structural stability of ligand-DAT complexes via low RMSD values and persistent interactions. These combined computational results suggest that compounds like Modafinil, Benztropine, and Procaine could be promising DAT radiotracers for imaging in Parkinson's disease.

6.3. Challenges for computational studies of transporters

In the reported studies, we highlighted that the major challenge in modeling transporter proteins is the presence of macro-conformational changes that these systems undergo to transport the substrate from one side of the membrane to the other. The success of the simulation and the reliability of the prediction are strictly linked to the availability of the 3D structure of the proper conformation. Furthermore, being membrane proteins, also transporter modeling needs to properly address the interaction with membrane components (see Section 3.11).

7. Disordered peptides

7.1. β-amyloid

Alzheimer's disease (AD) is a neurodegenerative disorder characterized by the irreversible loss of neurons, resulting in a gradual decline in cognitive function. It is commonly believed that AD is driven by abnormal protein dynamics, particularly the accumulation of β-amyloid in extracellular plaques and the breakdown of *tau* protein, forming neurofibrillary tangles inside cells. Extensive research suggests that the overproduction of β-amyloid peptides and their aggregation into plaques are closely linked to the early development of AD.

Consequently, non-invasive imaging techniques such as PET and SPECT are now being used to monitor amyloid pathology and facilitate the early detection of AD. Benzyloxybenzene based compounds labeled with ^{125}I were proposed as a novel flexible scaffold and evaluated as ligands toward amyloid plaques. Yang et al. [52,205] used three-dimensional quantitative structure–activity relationship (3D-QSAR) of benzyloxybenzene derivatives to clarify the interaction mechanism between the compounds and β-amyloid fibers. In detail, first a QM geometry optimization of the crystal structure conformation was performed in Gaussian09 using B3LYP/3-21G for iodine and B3LYP/6-31G for other atoms in the water phase. Then, a CoMFA [206] and CoMSIA [207] were computed. These two methods use statistical correlation techniques for the analysis of the quantitative relationship between the biological activity of a set of compounds with a specified alignment, and their three-dimensional electronic and steric properties.

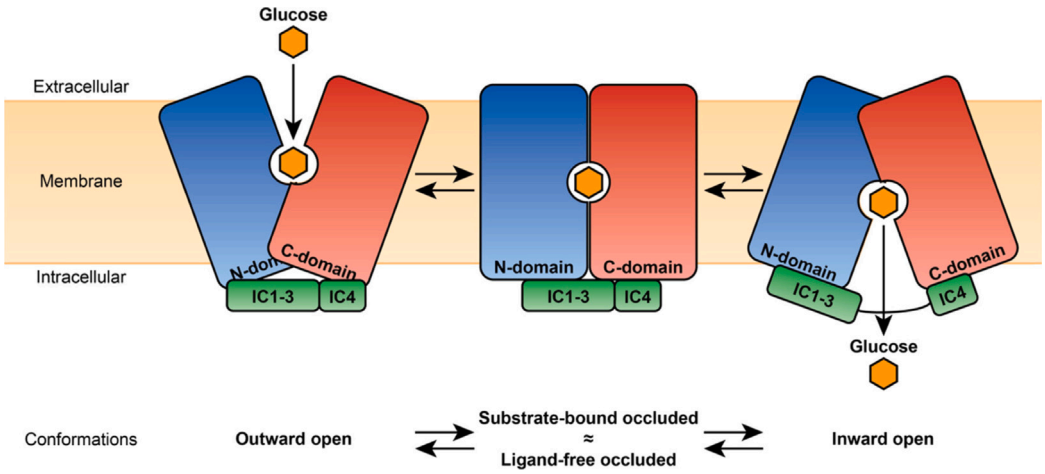

Fig. 8. GLUTs macro-conformation (outward-open, substrate-bound/ligand-free occluded, inward-open) required for a complete transport cycle according to the alternating access model.
Source: Reproduced with permission from Ref. [200].

7.2. α-sinuclein

Parkinson's disease and dementia with Lewy bodies are common neurodegenerative disorders, marked by progressive motor and cognitive decline. Both conditions are neuropathologically defined by the presence of Lewy bodies and Lewy neurites, primarily composed of aggregated α-synuclein. Abnormal α-synuclein is also a key element in the glial cytoplasmic inclusions found in multiple system atrophy, another neurodegenerative disorder that affects movement and autonomic functions. These disorders involve the formation of α-synuclein filaments with β-pleated sheet structures. Recent cryo-EM studies have shown that the ultrastructures of these filaments can vary both by disease type and between individuals [208]. Imaging techniques capable of detecting α-synuclein aggregates with high sensitivity would offer critical insights for early-stage disease diagnosis. Such methods could also be highly valuable in assessing the effectiveness of drug candidates aimed at targeting α-synuclein pathologies, both in preclinical and clinical stages of development. Computational investigation on this target is challenging, given the highly disordered structure of α-synuclein, and therefore the definition and sampling of an appropriate conformation of both the aggregates and the ligands. Starting from available experimental structure of filaments of α-synuclein, one strategy is to perform blind docking and identify putative binding hot-spots [209]. However, due to the intrinsic disorder of the fibrils and their high flexibility, MD simulations could be further needed.

Janssen et al. [53] performed blind docking of fluorinated compounds with AutoDock, generating 1000 poses per compound. The full-length α-synuclein fibril structure (PDB ID 2N0A [210]) was targeted, selected for its relevance and representativeness in early *in vitro* screening despite the availability of newer cryo-EM structures. To explore interactions of the α-synuclein fibril, molecular dynamics simulations were conducted using NAMD with the CHARMM22 force field. The binding pose with the best docking energy was selected for these simulations. The system, comprising the fibril core from Lys32 to Lys102 and the bound ligand, was solvated in a TIP3P water box and neutralized with sodium ions, and a 5 ns production run was performed.

Verdurand et al. [54] used the Site Finder program implemented in MOE to identify docking sites on fibril structures that previously underwent MD simulations. Then, the best docking poses underwent further simulations using the enhanced sampling technique umbrella sampling [211]. Umbrella sampling is a computational technique used in MD to enhance sampling along a specific reaction coordinate by applying a series of biased potentials, allowing for accurate estimation of free energy profiles across energy barriers that are otherwise difficult to sample efficiently. In Verdurand work, umbrella sampling simulations were carried out using 220 windows, with the center-of-mass distance between the tracer and protein atoms ranging from 27 to 5.1 Å, spaced at 0.1 Å intervals. A harmonic potential with a force constant of 25 kcal/mol· $Å^2$ was applied in each window to maintain these distances. Positional restraints were also applied to the backbone atoms of proteins located at the fibril edges and those involved in the reaction coordinate. Each window underwent 40 ps of equilibration followed by 100 ps of production simulation. To derive the free energy profile along the reaction coordinate, the weighted histogram analysis method (WHAM) [212] was used to process the biased probability distributions obtained from the simulations. They identified a deeply buried interaction site within the α-synuclein structure, suggesting that candidate molecules must penetrate the structure between the strand ladders to reach the interaction site.

7.3. Challenges for computational studies of disordered proteins

The clear challenge regarding the modeling of disordered proteins is their intrinsic high flexibility. This often leads to the lack of a defined secondary structure, to the presence of wide surfaces instead of binding pockets, and high exposure to the solvent, that make these proteins undruggable. As a result, blind docking or specific software to identify binding hot-spots are often used, usually followed by MD simulations.

8. Molecular databases for machine learning

Artificial intelligence (AI) is revolutionizing drug design and discovery by rapidly analyzing vast datasets, identifying promising drug candidates, and optimizing molecular structures. AI-driven algorithms, such as deep learning and generative models, enhance virtual screening, structure-based drug design, and *de novo* molecule generation. Molecular databases serve as the foundation for AI applications, providing extensive libraries of chemical structures, bioactivity data, and pharmacokinetic properties that fuel machine learning models. The integration of AI with molecular databases enables efficient prediction of drug–target interactions, accelerating the identification of novel radiopharmaceutical compounds [213,214]. Molecular databases store vast quantities of scientific data, including MD simulation-derived data as in the case of MDDB [215], paving the way for bioinformatics and chemoinformatics studies [216–220]. The importance of these tools has pushed the collection of an extensive array of databases and web-based resources [12,221–223]. In this context, besides structure-based drug design, a useful strategy to study radiopharmaceutical

is ligand-based drug design, where molecular databases play a key role, supplying molecular structures, force fields, and descriptors. In particular, descriptors can be used for QSAR or machine learning studies [224].

Öztürk et al. [6] focused on the critical role of metal-based radiopharmaceuticals in cancer diagnosis and therapy. As mentioned before, these compounds consist of a radiometal–chelator moiety attached to a biovector targeting specific biological markers, such as proteins overexpressed in tumors. The effectiveness and stability of these drugs depend on the compatibility between the radiometal and the chelator, which requires careful consideration of factors like oxidation state, ionic radius, and coordination geometry. The study analyzed 120 radiometal–chelator complexes, involving 25 radiometals and 30 chelators, using data from the CSD. Advanced QM and MD simulations were employed to evaluate electronic and dynamic properties, generating Amber force field parameters and molecular descriptors. These tools were rigorously validated and tested, ensuring reliability. The study makes the molecular descriptors and parameters publicly accessible, supporting their application in predictive modeling, molecular dynamics, and drug design.

Bamdi et al. [225] highlighted the use of Quantitative Structure–Property Relationships (QSPR) to predict the LogP for 121 radiopharmaceutical molecules. By employing a hybrid optimal descriptor that integrates SMILES representations and hydrogen-suppressed graphs, QSPR models were constructed and evaluated. These models indicated the structural factors that promote increases or decreases in LogP, offering valuable insights for optimizing molecular properties in radiopharmaceutical development.

Cheng et al. [226] introduced SATCMF (Structure-Aware Transformer Combined with Molecular Fingerprint), a novel graph transformer framework that incorporates chemical knowledge to model interactions between chelators and metal ions. The dataset used to train the models was primarily sourced from the IUPAC Stability Constants Database (SC-database) [227], which compiles experimentally reported dissociation, binding, and stability constants for metal ion–ligand interactions. As the SC-database is no longer actively maintained, the dataset was supplemented with manually curated data from recent literature to ensure broader coverage. The authors standardized all molecular structures using RDKit [228] to facilitate the generation of molecular fingerprints and their transformation into graph-based representations. Trained on stability data from metal–ligand complexes, SATCMF uses the SAT network to capture structural binding features and integrates molecular fingerprints to enhance the prediction of stability constants.

9. Challenges and future perspectives

The reported studies highlighted several challenges and solutions related to the specific targets. However, some challenges are common to the modeling and simulation of radiopharmaceuticals. One of these challenges is the proper treatment of metal-containing compounds, in this case the radionuclides, that own the unique nature of transition metal coordination chemistry. Unlike conventional drugs, metallodrugs can involve multiple oxidation and spin states, variable coordination numbers and geometries, and phenomena such as Jahn-Teller distortions and back-bonding. This represents an issue both for simplified methods like molecular docking (where in most cases the metal ion is completely neglected), and for more advances techniques, like MD simulations. Classical force fields (*e.g.*, Amber, CHARMM) struggle to accurately represent these flexible and labile metal–ligand interactions, sometimes failing to capture ligand exchange or changes in coordination geometry important for metal complexes. Polarizable force fields like AMOEBA offer some improvements but at substantial computational cost. QM methods, including *ab initio* and DFT, provide accurate structural and energetic descriptions but are limited by high computational demands and small system sizes. Hybrid QM/MM approaches combine quantum accuracy at the metal center with classical treatment of the environment, balancing computational feasibility with precision. Additional complexities arise from radionuclide decay effects, radiation-induced bond breakage, and the need to model bifunctional chelators' impact on drug–target binding [16,229,230]. All of these properties reflect on the pairing of radionuclides with the chelators. For this reason, when predicting the binding between a radiopharmaceutical and a protein, the correct ionization and coordination geometry of the chelator should be properly considered, even if the radionuclide has been neglected from the simulation (for instance, for parameterization issues). This can be achieved, for both docking and MD simulation, first, with a conformational study on the complete radiopharmaceutical, possibly at the QM level. Then, applying conformational restraints to the optimized geometry. This protocol should also be followed in the case of a peptide-based radiodrug, with additional care for the choice of the peptide conformation. Given their higher flexibility, peptides need a more thoughtful sampling of their conformations, which can be done using geometrical conformational sampling or through MD simulations. Overall, the future direction indicated by recent studies on the design of new radiopharmaceuticals seems to be the use of hybrid and combined computational approaches, and the development of multimeric or bifunctional radiopharmaceuticals, which allow for increased target affinity.

Besides the strategies to increase protein–ligand affinity, another challenge regards the pharmacokinetics of radiopharmaceuticals, that need to reach the targeting site without being metabolized first, and need to be non-toxic. In this regard, an emerging field in radiopharmaceutical design involves multifunctional nanoplatforms that integrate diagnostic imaging, targeted therapy, and drug delivery within a single construct, enhancing tumor accumulation via the enhanced permeability and retention effect and active ligand–receptor targeting [231]. Organic platforms like liposomes, dendrimers (*e.g.*, PAMAM), and polymeric micelles (PLGA, PEG-based) offer superior biocompatibility, biodegradability, and controlled release of radionuclides such as ^{177}Lu, ^{64}Cu, or ^{225}Ac [232], alongside chemotherapeutics like doxorubicin, achieving high tumor retention and reduced immunogenicity. Inorganic platforms, including gold nanoparticles (AuNPs), quantum dots, superparamagnetic iron oxide nanoparticles (SPIONs), and mesoporous silica nanoparticles (MSNs), provide structural robustness, multimodal imaging (PET/MRI), and radiosensitization; examples include ^{64}Cu-doped AuNPs for PET and ^{177}Lu-MSNs for synergistic chemoradiotherapy. Hybrid systems, such as dendrimer–AuNP conjugates or CuS@MSN yolk-shell structures, merge these strengths with metal cores for photothermal enhancement and porous frameworks for high payload capacity, optimizing pharmacokinetics like extended half-life and precise cellular uptake [231,233,234]. Besides nuclear radiations, optical imaging can be exploited to generate high-resolution images of biological structures (*e.g.*, fluorescence, or Cerenkov radiation) [235]. Therefore, thanks to the increasing computational power, *in silico* simulations can contribute to the development of probes in this promising area.

MD simulations, quantum mechanics, docking, and machine learning elucidate organic, inorganic and hybrid platform interactions with drugs, biomolecules, and lipid membranes, revealing how surface charge, lipid composition (*e.g.*, phosphatidylglycerol), and morphology (nanorods, nanostars) govern electrostatic-driven uptake via endocytosis or phagocytosis. These models predict optimized peptide conjugation, drug loading, and stability, while AI-driven neural networks forecast patient-specific biodistribution, therapeutic efficacy, and reduced toxicity. Collectively, such platforms improve radiopharmaceutical precision by boosting stability, target specificity, and multimodal theranostics [236–238].

10. Conclusions

Computational approaches have become indispensable tools in the development of radiopharmaceuticals, offering invaluable insights into

the knowledge of detailed molecular interactions, overall stability of the systems, and estimates of binding affinities. The integration of molecular docking, MD simulations, and QM calculations has significantly improved the rational design of radiopharmaceuticals, enabling the optimization of ligands for a broad class of targets such as receptors, enzymes, and transporters. By elucidating the structural dynamics of biomolecular targets such as GPCRs, enzymes like PSMA and FAP, and transporters such as GLUTs, computational studies have guided the design of more effective and selective therapeutics and/or diagnostic agents. A key advantage of computational studies is their ability to predict binding modes and affinities with high precision, reducing the need for extensive trial-and-error experimental approaches. Advances in these methodologies have enabled the study of non-standard radiometals, thus overcoming challenges associated with parameterization in commonly used force fields. Additionally, the role of molecular databases in facilitating ligand-based drug design has expanded, supporting predictive modeling and virtual screening for novel radiopharmaceutical candidates. Despite these advancements, several challenges still remain. The accurate simulation of radionuclide-containing molecules, the dynamic behavior of flexible peptides, and the influence of chelator moieties on binding efficacy require further development and refinement of computational techniques. Additionally, the increasing use of machine learning models and AI-driven approaches holds promise in accelerating the discovery and optimization of next-generation theranostic agents. Ultimately, these advancements will contribute to improved patient outcomes by enabling more precise and personalized nuclear medicine applications.

CRediT authorship contribution statement

Silvia Gervasoni: Writing – review & editing, Writing – original draft, Visualization, Investigation. **Camilla Guccione:** Writing – original draft, Visualization, Investigation. **Giuliano Malloci:** Writing – review & editing, Supervision, Project administration.

Declaration of competing interest

The authors declare the following financial interests/personal relationships which may be considered as potential competing interests: Silvia Gervasoni reports financial support was provided by Italian Ministry of University and Research. If there are other authors, they declare that they have no known competing financial interests or personal relationships that could have appeared to influence the work reported in this paper.

Acknowledgment

The authors gratefully acknowledge the Health Extended ALliance for Innovative Therapies, Advanced Lab-research, and Integrated Approaches of Precision Medicine partnership (HEAL ITALIA), founded by the Italian Ministry of University and Research, PNRR, mission 4, component 2, investment 1.3, project number PE00000019 (University of Cagliari).

Data availability

No data was used for the research described in the article.

References

[1] S. Chaturvedi, A.K. Mishra, Small molecule radiopharmaceuticals – a review of current approaches, Front. Med. 3 (5) (2016) http://dx.doi.org/10.3389/fmed.2016.00005, eCollection.

[2] E. Boros, A.B. Packard, Radioactive transition metals for imaging and therapy, Chem. Rev. 119 (2) (2019) 870–901, http://dx.doi.org/10.1021/acs.chemrev.8b00281.

[3] T.I. Kostelnik, C. Orvig, Radioactive main group and rare earth metals for imaging and therapy, Chem. Rev. 119 (2) (2019) 902–956, http://dx.doi.org/10.1021/acs.chemrev.8b00294.

[4] S. Zhang, X. Wang, X. Gao, X. Chen, L. Li, G. Li, C. Liu, Y. Miao, R. Wang, K. Hu, Radiopharmaceuticals and their applications in medicine, Sig. Transduct. Target. Ther. 10 (2025) 1, http://dx.doi.org/10.1038/s41392-024-02041-6.

[5] X. Wang, C. Chen, J. Yan, Y. Xu, D. Pan, L. Wang, M. Yang, Druggability of targets for diagnostic radiopharmaceuticals, ACS Pharmacol. Transl. Sci. 6 (8) (2023) 1107–1119, http://dx.doi.org/10.1021/acsptsci.3c00081.

[6] I. Öztürk, S. Gervasoni, C. Guccione, A. Bosin, A.V. Vargiu, P. Ruggerone, G. Malloci, Force fields, quantum-mechanical- and molecular-dynamics-based descriptors of radiometal–chelator complexes, Molecules 29 (18) (2024) 4416, http://dx.doi.org/10.3390/molecules29184416.

[7] S. Dhoundiyal, S. Srivastava, S. Kumar, G. Singh, S. Ashique, R. Pal, N. Mishra, F. Taghizadeh-Hesary, Radiopharmaceuticals: navigating the frontier of precision medicine and therapeutic innovation, Eur. J. Med. Res. 29 (2024) 26, http://dx.doi.org/10.1186/s40001-023-01627-0.

[8] U. Hennrich, K. Kopka, Lutathera®: The first fda- and ema-approved radiopharmaceutical for peptide receptor radionuclide therapy, Pharmaceuticals 12 (3) (2019) 114, http://dx.doi.org/10.3390/ph12030114.

[9] E. Merola, C.M. Grana, Peptide receptor radionuclide therapy (prrt): Innovations and improvements, Cancers 15 (11) (2023) 2975, http://dx.doi.org/10.3390/cancers15112975.

[10] M. Shabsigh, L.A. Solomon, Peptide pet imaging: A review of recent developments and a look at the future of radiometal-labeled peptides in medicine, Chem. Biomed. Imaging 2 (9) (2024) 615–630, http://dx.doi.org/10.1021/cbmi.4c00030.

[11] Y. Xu, J. Zhang, D. Pan, J. Yan, C. Chen, L. Wang, X. Wang, M. Yang, Y. Xu, Development of novel peptide-based radiotracers for detecting fgl1 expression in tumors, Mol. Pharm. 22 (3) (2025) 1605–1614, http://dx.doi.org/10.1021/acs.molpharmaceut.4c01293.

[12] A. Macorano, A. Mazzolari, G. Malloci, A. Pedretti, G. Vistoli, S. Gervasoni, An improved dataset of force fields, electronic and physicochemical descriptors of metabolic substrates, Sci. Data 11 (2024) 929, http://dx.doi.org/10.1038/s41597-024-03707-0.

[13] L. Chang, A. Mondal, A. Perez, Towards rational computational peptide design, Front. Bioinform. 2 (2022) 1046493, http://dx.doi.org/10.3389/fbinf.2022.1046493.

[14] V. Patamia, C. Zagni, I. Brullo, E. Saccullo, A. Coco, G. Floresta, A. Rescifina, Computer-assisted design of peptide-based radiotracers, Int. J. Mol. Sci. 24 (7) (2023) 6856, http://dx.doi.org/10.3390/ijms24076856.

[15] G. Sgouros, L. Bodei, M.R. McDevitt, J.R. Nedrow, Radiopharmaceutical therapy in cancer: clinical advances and challenges, Nat. Rev. Drug Discov. 19 (2020) 589–608, http://dx.doi.org/10.1038/s41573-020-0073-9.

[16] S.E. Lapi, P.J. Scott, A.M. Scott, A.D. Windhorst, B.M. Zeglis, M. Abdel-Wahab, R.P. Baum, J.M. Buatti, F. Giammarile, A.P. Kiess, A. Jalilian, P. Knoll, A. Korde, J. Kunikowska, S.T. Lee, D. Paez, J.-L. Urbain, J. Zhang, J.S. Lewiss, Recent advances and impending challenges for the radiopharmaceutical sciences in oncology, Lancet Oncol. 25 (6) (2024) e236–e249, http://dx.doi.org/10.1016/S1470-2045(24)00030-5.

[17] T.P. Varghese, A. John, J. Mathew, Revolutionizing cancer treatment: The role of radiopharmaceuticals in modern cancer therapy, Precis. Radiat. Oncol. 8 (3) (2024) 145–152, http://dx.doi.org/10.1002/pro6.1239.

[18] M. Salahinejad, D.A. Winkler, F. Shiri, Discovery and design of radiopharmaceuticals by in silico methods, Curr. Radiopharm. 15 (4) (2022) 271–319, http://dx.doi.org/10.2174/1874471015666220831091403.

[19] I.M. Jackson, E.W. Webb, P.J. Scott, M.L. James, In silico approaches for addressing challenges in cns radiopharmaceutical design, ACS Chem. Neurosci. 13 (12) (2022) 1675–1683, http://dx.doi.org/10.1021/acschemneuro.2c00269.

[20] J. Tao, L. Liang, S. Hao, Y. Chen, Z. Yang, Y. Cai, H. Zhu, Artificial intelligence for radiopharmaceutical and molecular imaging, Acta Pharm. Sin. B (2025) 2211–3835, http://dx.doi.org/10.1016/j.apsb.2025.09.039.

[21] B. Ataeinia, P. Heidari, Artificial intelligence and the future of diagnostic and therapeutic radiopharmaceutical development: in silico smart molecular design, PET Clin. 16 (4) (2022) 513–523, http://dx.doi.org/10.1016/j.cpet.2021.06.008.

[22] Z. Cai, Q. Ouyang, D. Zeng, K.N. Nguyen, J. Modi, L. Wang, A.G. White, B.E. Rogers, X.-Q. Xie, C.J. Anderson,^{64}cu-labeled somatostatin analogues conjugated with cross-bridged phosphonate-based chelators via strain-promoted click chemistry for pet imaging: In silico through in vivo studies, J. Med. Chem. 57 (14) (2014) 6019–6029, http://dx.doi.org/10.1021/jm500416f.

[23] S. Gervasoni, I. Öztürk, C. Guccione, A. Bosin, P. Ruggerone, G. Malloci, Interaction of radiopharmaceuticals with somatostatin receptor 2 revealed by molecular dynamics simulations, J. Chem. Inf. Model. 63 (15) (2023) 4924–4933, http://dx.doi.org/10.1021/acs.jcim.3c00712.

[24] P.F.J. Lipiński, P. Garnuszek, M. Maurin, R. Stoll, N. Metzler-Nolte, A. Wodyński, J.C. Dobrowolski, M.K. Dudek, M. Orzełowska, R. Mikołajczak, Structural studies on radiopharmaceutical dota-minigastrin analogue (cp04) complexes and their interaction with cck2 receptor, EJNMMI Res. 8 (2018) 33, http://dx.doi.org/10.1186/s13550-018-0387-3.

[25] C. Liolios, C. Patsis, G. Lambrinidis, E. Tzortzini, M. Roscher, U. Bauder-Wüst, A. Kolocouris, K. Kopka, Investigation of tumor cells and receptor–ligand simulation models for the development of pet imaging probes targeting psma and grpr and a possible crosstalk between the two receptors, Mol. Pharm. 19 (7) (2022) 2231–2247, http://dx.doi.org/10.1021/acs.molpharmaceut.2c00070.

[26] S.N. Moldovean, D.G. Timaru, V. Chiș, All-atom molecular dynamics investigations on the interactions between d2 subunit dopamine receptors and three^{11}c-labeled radiopharmaceutical ligands, Int. J. Mol. Sci. 23 (4) (2022) 2005, http://dx.doi.org/10.3390/ijms23042005.

[27] R.R. Luedtke, Y. Mishra, Q. Wang, S.A. Griffin, C. Bell-Horner, M. Taylor, S. Vangveravong, G.H. Dillon, R.-Q. Huang, D.E. Reichert, R.H. Mach, Comparison of the binding and functional properties of two structurally different d2 dopamine receptor subtype selective compounds, ACS Chem. Neurosci. 3 (12) (2012) 1050–1062, http://dx.doi.org/10.1021/cn300142q.

[28] O. Demmer, I. Dijkgraaf, U. Schumacher, L. Marinelli, S. Cosconati, E. Gourni, H.-J. Wester, H. Kessle, Design, synthesis, and functionalization of dimeric peptides targeting chemokine receptor cxcr4, J. Med. Chem. 54 (21) (2011) 7648–7662, http://dx.doi.org/10.1021/jm2009716.

[29] R.H. Gaonkar, Y.T. Schmidt, R. Mansi, Y. Almeida-Hernandez, E. Sanchez-Garcia, M. Harms, J. Münch, M. Fani, Development of a new class of cxcr4-targeting radioligands based on the endogenous antagonist epi-x4 for oncological applications, J. Med. Chem. 66 (13) (2023) 8484–8497, http://dx.doi.org/10.1021/acs.jmedchem.3c00131.

[30] J. Matalińska, K. Kosińska, P.K. Halik, P. Koźmiński, P.F.J. Lipiński, E. Gniazdowska, A. Misicka, Novel nk1r-targeted^{68}ga-/^{177}lu-radioconjugates with potential application against glioblastoma multiforme: Preliminary exploration of structure–activity relationships, Int. J. Mol. Sci. 23 (3) (2022) 1214, http://dx.doi.org/10.3390/ijms23031214.

[31] L. Xie, L. Zhang, K. Hu, M. Hanyu, Y. Zhang, M. Fujinaga, K. Minegishi, T. Ohkubo, K. Nagatsu, C. Jiang, T. Shimokawa, K. Ashisuke, N. Okonogi, S. Yamada, F. Wang, R. Wang, M.-R. Zhang, A^{211}at-labelled mglur1 inhibitor induces cancer senescence to elicit long-lasting anti-tumor efficacy, Cell Rep. Med. 4 (4) (2023) 100960, http://dx.doi.org/10.1016/j.xcrm.2023.100960.

[32] Y. Li, K. Dahl, P. Johnström, K. Varnäs, L. Farde, C. Halldin, A. Medd, D. Maier, M.E. Powell, J. Chen, R. Van, J. Patel, A. Chaudhary, Y. Gao, Z. Song, A. Haider, Y. Shao, C.S. Elmore, S. Liang, M. Schou, Radiosynthesis and evaluation of 11c-labeled isoindolone-based positive allosteric modulators for positron emission tomography imaging of metabotropic glutamate receptor 2, ACS Pharmacol. Transl. Sci. 7 (8) (2024) 2414–2423, http://dx.doi.org/10.1021/acsptsci.4c00261.

[33] A.K. Sharma, R. Sharma, A. Das, A. Chakraborty, S. Rakshit, H.D. Sarma, A. Mukherjee, T. Das, D. Satpati, Synthesis and 177lu labeling of the first retro analog of the her2-targeting a9 peptide: A superior variant, Bioconjugate Chem. 34 (9) (2023) 1576–1584, http://dx.doi.org/10.1021/acs.bioconjchem.3c00265.

[34] M.A. Binmujlli, Radioiodinated anastrozole and epirubicin for her2-targeted cancer therapy: Molecular docking and dynamics insights with implications for nuclear imaging, Processes 12 (8) (2024) 1659, http://dx.doi.org/10.3390/pr12081659.

[35] N. Pirooznia, K. Abdi, D. Beiki, F. Emami, S.S. Arab, O. Sabzevari, Z. Pakdin-Parizi, P. Geramifar, Radiosynthesis, biological evaluation, and preclinical study of a 68ga-labeled cyclic rgd peptide as an early diagnostic agent for overexpressed $\alpha v\beta 3$ integrin receptors in non-small-cell lung cancer, Mol. Imaging 8421657 (2020) 11, http://dx.doi.org/10.1155/2020/8421657.

[36] L. Chen, H. Fu, W. Li, Q. Shen, Y. Luo, J. Fu, C. Shao, H. He, K. Lou, J. Wang, G. Feng, C. Yu, Development and preclinical evaluation of a cyclic pet tracer targeting integrin-$\alpha 6$ on colorectal cancer models, Bioorg. Chem. 153 (2024) 107892, http://dx.doi.org/10.1016/j.bioorg.2024.107892.

[37] S.H. Lee, N. Denora, V. Laquintana, G.F. Mangiatordi, A. Lopedota, A. Lopalco, A. Cutrignelli, M. Franco, P. Delre, I.H. Song, H.W. Kim, S.B. Kim, H.S. Park, K. Kim, S.-Y. Lee, H. Youn, B.C. Lee, S.E. Kim, Radiosynthesis and characterization of [18f]bs224: a next-generation tspo pet ligand insensitive to the rs6971 polymorphism, Eur. J. Nucl. Med. Mol. Imaging 49 (1) (2021) 110–124, http://dx.doi.org/10.1007/s00259-021-05617-4.

[38] X. Wang, Y. Chen, Y. Xiong, L. Zhang, B. Wang, Y. Liu, M. Cui, Design and characterization of squaramic acid–based prostate-specific membrane antigen inhibitors for prostate cancer, J. Med. Chem. 66 (10) (2023) 6889–6904, http://dx.doi.org/10.1021/acs.jmedchem.3c00309.

[39] C. Liolios, D. Bouziotis, W. Sihver, M. Schäfer, G. Lambrinidis, E.-A. Salvanou, U. Bauder-Wüst, M. Benesova, K. Kopka, A. Kolocouris, et al., Synthesis and preclinical evaluation of a bispecific psma-617/rm2 heterodimer targeting prostate cancer, ACS Med. Chem. Lett. 15 (11) (2024) 1970–1978.

[40] A. Galbiati, M. Bocci, S. Gervasoni, E. Prodi, G. Malloci, D. Neri, S. Cazzamalli, Molecular evolution of multivalent oncofap derivatives with enhanced tumor uptake and prolonged tumor retention, J. Med. Chem. 67 (15) (2024) 13392–13408, http://dx.doi.org/10.1021/acs.jmedchem.4c01295.

[41] L. Li, R. Cao, K. Chen, C. Qu, K. Qian, J. Lin, R. Li, C. Lai, X. Wang, Z. Han, Z. Xu, L. Zhou, S. Song, W. Zhu, Z. Cheng, Development of an fap-targeted pet probe based on a novel quinolinium molecular scaffold, Bioconjugate Chem. 35 (9) (2024) 1309–1317, http://dx.doi.org/10.1021/acs.bioconjchem.4c00214.

[42] D. Fatehi, Z. Hajimahdi, M. Mosayebnia, Pioneering qsar modeling study of fap-targeting radiopharmaceuticals used in oncology, Chem. Biol. Drug. Des. 106 (4) (2025) e70177, http://dx.doi.org/10.1111/cbdd.70177.

[43] S. Chatterjee, W.G. Lesniak, M.S. Miller, A. Lisok, E. Sikorska, B. Wharram, D. Kumar, M. Gabrielson, M.G. Pomper, S.B. Gabelli, S. Nimmagadda, Rapid pd-l1 detection in tumors with pet using a highly specific peptide, Biochem. Biophys. Res. Commun. 483 (2017) 258–263, http://dx.doi.org/10.1016/j.bbrc.2016.12.156.

[44] H. Kuan, H. Masayuki, L. Xie, Y. Zhang, N. Kotaro, S. Hisashi, M.-R. Zhang, Developing native peptide-based radiotracers for pd-l1 pet imaging and improving imaging contrast by pegylatione, Chem. Commun. 55 (29) (2019) 4273, http://dx.doi.org/10.1039/c9cc90113b.

[45] S. Ge, B. Zhang, J. Li, J. Shi, T. Jia, Y. Wang, Z. Chen, S. Sang, S. Deng, A novel 68ga-labeled cyclic peptide molecular probe based on the computer-aided design for noninvasive imaging of pd-l1 expression in tumors, Bioorg. Chem. 140 (2023) 106785, http://dx.doi.org/10.1016/j.bioorg.2023.106785.

[46] M. Zhou, X. Wang, B. Chen, S. Xiang, W. Rao, Z. Zhang, H. Liu, J. Fang, X. Yin, P. Deng, X. Zhang, S. Hu, Preclinical and first-in-human evaluation of 18f-labeled d-peptide antagonist for pd-l1 status imaging with pet, Eur. J. Nucl. Med. Mol. Imaging 49 (2022) 4312–4324, http://dx.doi.org/10.1007/s00259-022-05876-9.

[47] G. Ferro-Flores, B. Ocampo-García, P. Cruz-Nova, M. Luna-Gutiérrez, G. Bravo-Villegas, E. Azorín-Vega, N. Jiménez-Mancilla, E. Michel-Sánchez, O. García-Pérez, N. Lara-Almazán, C. Santos-Cuevas, 99Mtc-labeled cyclic peptide targeting pd-l1 as a novel nuclear imaging probe, Pharmaceutics 15 (12) (2023) 2662, http://dx.doi.org/10.3390/pharmaceutics15122662.

[48] G. Ferro-Flores, M. Luna-Gutiérrez, B. Ocampo-García, N. Jiménez-Mancilla, N. Lara-Almazán, R. Oros-Pantoja, C. Santos-Cuevas, E. Azorín-Vega, L. Meléndez-Alafort, Synthesis and evaluation of [18f]alf-nota-ipd-l1 as a potential theranostic pair for [177lu]lu-dota-ipd-l1, Pharmaceutics 17 (7) (2025) 920, http://dx.doi.org/10.3390/pharmaceutics17070920.

[49] M. Luna-Gutiérrez, E. Azorín-Vega, R. Oros-Pantoja, B. Ocampo-García, P. Cruz-Nova, N. Jiménez-Mancilla, G. Bravo-Villegas, C. Santos-Cuevas, L. Meléndez-Alafort, G. Ferro-Flores, Lutetium-177 labeled ipd-l1 as a novel immunomodulator for cancer-targeted radiotherapy, EJNMMI Radiopharm. Chem. 10 (5) (2025) 1–23, http://dx.doi.org/10.1186/s41181-025-00328-9.

[50] N. Rana, M.A. Aziz, A.K. Oraby, M. Wuest, J. Dufour, K.A.M. Abouzid, F. Wuest, F.G. West, Towards selective binding to the glut5 transporter: Synthesis, molecular dynamics and in vitro evaluation of novel c-3-modified 2 5-anhydro-d-mannitol analogs, Pharmaceutics 14 (4) (2022) 828, http://dx.doi.org/10.3390/pharmaceutics14040828.

[51] J.A. Castillo-Garit, M. Soria-Merino, K. Mena-Ulecia, M. Romero-Otero, V. Pérez-Doñate, F. Torrens, F. Pérez-Giménez, Combining qsar and molecular docking for the methodological design of novel radiotracers targeting parkinson's disease, Appl. Sci. 15 (15) (2025) 8134, http://dx.doi.org/10.3390/app15158134.

[52] Y. Yang, X. Zhang, M. Cui, J. Zhang, Z. Guo, Y. Li, X. Zhang, J. Dai, B. Liu, Preliminary characterization and in vivo studies of structurally identical 18f- and 125i-labeled benzyloxybenzenes for pet/spect imaging of β-amyloid plaques, Sci. Rep. 5 (2015) 12084, http://dx.doi.org/10.1038/srep12084.

[53] B. Janssen, G. Tian, Z. Lengyel-Zhand, C.-J. Hsieh, M.G. Lougee, A. Riad, K. Xu, C. Hou, C.-C. Weng, B.J. Lopresti, H.J. Kim, V.V. Pagar, J.J. Ferrie, B.A. Garcia, C.A. Mathis, K. Luk, E.J. Petersson, R.H. Mach, Identification of a putative α-synuclein radioligand using an in silico similarity search, Mol. Imaging. Biol. 25 (2023) 704–719, http://dx.doi.org/10.1007/s11307-023-01814-9.

[54] M. Verdurand, E. Levigoureux, W. Zeinyeh, L. Berthier, M. Mendjel-Herda, F. Cadarossanesaib, C. Bouillot, T. Iecker, R. Terreux, S. Lancelot, F. Chauveau, T. Billard, L. Zimmer, In silico, in vitro, and in vivo evaluation of new candidates for α-synuclein pet imaging, Mol. Pharm. 15 (8) (2018) 3153–3166, http://dx.doi.org/10.1021/acs.molpharmaceut.8b00229.

[55] J. Li, T. Zhao, Q. Yang, S. Du, L. Xu, A review of quantitative structure–activity relationship: The development and current status of data sets, molecular descriptors and mathematical models, Chemom. Intell. Lab. Syst. 256 (2025) 105278, http://dx.doi.org/10.1016/j.chemolab.2024.105278.

[56] T. Hameduh, Y. Haddad, V. Adam, Z. Heger, Homology modeling in the time of collective and artificial intelligence, Comput. Struct. Biotechnol. J. 18 (2020) 3494–3506, http://dx.doi.org/10.1016/j.csbj.2020.11.007.

[57] L. Pinzi, G. Rastelli, Molecular docking: Shifting paradigms in drug discovery, Int. J. Mol. Sci. 20 (18) (2019) 4331, http://dx.doi.org/10.3390/ijms20184331.

[58] J.D. Durrant, J.A. McCammon, Molecular dynamics simulations and drug discovery, BMC Biol. 9 (2011) 71, http://dx.doi.org/10.1186/1741-7007-9-71.

[59] E. King, E. Aitchison, H. Li, R. Luo, Recent developments in free energy calculations for drug discovery, Front. Mol. Biosci. 8 (2021) 712085, http://dx.doi.org/10.3389/fmolb.2021.712085.

[60] K. Sriram, P.A. Insel, G protein-coupled receptors as targets for approved drugs: How many targets and how many drugs? Mol. Pharmacol. 93 (4) (2018) 251–258, http://dx.doi.org/10.1124/mol.117.111062.

[61] D. Yang, Q. Zhou, V. Labroska, S. Qin, S. Darbalaei, Y. Wu, E. Yuliantie, L. Xie, H. Tao, J. Cheng, Q. Liu, S. Zhao, W. Shui, Y. Jiang, M.-W. Wang, G protein-coupled receptors: structure- and function-based drug discovery, Sig. Transduct. Target. Ther. 6 (2021) 7, http://dx.doi.org/10.1038/s41392-020-00435-w.

[62] M. Colom, B. Vidal, L. Zimmer, Is there a role for gpcr agonist radiotracers in pet neuroimaging? Front. Mol. Neurosci. 12 (2019) 255, http://dx.doi.org/10.3389/fnmol.2019.00255.

[63] M. Zhang, T. Chen, X. Lu, X. Lan, Z. Chen, S. Lu, G protein-coupled receptors (gpcrs): advances in structures, mechanisms and drug discovery, Sig. Transduct. Target. Ther. 9 (2024) 88, http://dx.doi.org/10.1038/s41392-024-01803-6.

[64] D.N. Wiseman, A. Otchere, J.H. Patel, R. Uddin, N.L. Pollock, S.J. Routledge, A.J. Rothnie, C. Slack, D.R. Poyner, R.M. Bill, A.D. Goddard, Expression and purification of recombinant g protein-coupled receptors: A review, Protein Expr. Purif. 167 (2020) 105524, http://dx.doi.org/10.1016/j.pep.2019.105524.

[65] M.J. Robertson, J.G. Meyerowitz, O. Panova, K. Borrelli, G. Skiniotis, Plasticity in ligand recognition at somatostatin receptors, Nat. Struct. Mol. Biol. 29 (3) (2022) 210–217, http://dx.doi.org/10.1038/s41594-022-00727-5.

[66] S. Gervasoni, C. Guccione, V. Fanti, A. Bosin, G. Cappellini, B. Golosio, P. Ruggerone, G. Malloci, Molecular simulations of sstr2 dynamics and interaction with ligands, Sci. Rep. 13 (2023) 4768, http://dx.doi.org/10.1038/s41598-023-31823-1.

[67] C. Guccione, S. Gervasoni, I. Öztürk, A. Bosin, P. Ruggerone, G. Malloci, Exploring key features of selectivity in somatostatin receptors through molecular dynamics simulations, Comput. Struct. Biotechnol. J. 23 (2024) 1311–1319, http://dx.doi.org/10.1016/j.csbj.2024.03.005.

[68] A.N. Jain, Surflex: fully automatic flexible molecular docking using a molecular similarity-based search engine, J. Med. Chem. 46 (4) (2003) 499–511.

[69] D. Zeng, Q. Ouyang, Z. Cai, X.-Q. Xie, C.J. Anderson, New cross-bridged cyclam derivative cb-te1k1p, an improved bifunctional chelator for copper radionuclides, Chem. Commun. (Camb) 50 (1) (2014) 43–45, http://dx.doi.org/10.1039/c3cc45928d.

[70] A. Thompson, W. Liu, E. Chun, V. Katritch, H. Wu, E. Vardy, X. Huang, C. Trapella, R. Guerrini, G. Calo, B. Roth, V. Cherezov, R. Stevens, Structure of the nociceptin/orphanin fq receptor in complex with a peptide mimetic, Nature 485 (2012) 395–399, http://dx.doi.org/10.1038/nature11085.

[71] A. Manglik, A. Kruse, T. Kobilka, F. Thian, J. Mathiesen, R. Sunahara, L. Pardo, W. Weis, B. Kobilka, S. Granier, Crystal structure of the mu-opioid receptor bound to a morphinan antagonist, Nature 485 (2012) 321–326, http://dx.doi.org/10.1038/nature10954.

[72] H. Wu, D. Wacker, M. Mileni, V. Katritch, G.W. Han, E. Vardy, W. Liu, A.A. Thompson, X.-P. Huang, F.I. Carroll, S.W. Mascarella, R.B. Westkaemper, P.D. Mosier, B.L. Roth, V. Cherezov, R.C. Stevens, Structure of the human kappa-opioid receptor in complex with jdtic, Nature 485 (2012) 327–332, http://dx.doi.org/10.1038/nature10939.

[73] S. Granier, A. Manglik, A. Kruse, T. Kobilka, F. Thian, W. Weis, B. Kobilka, Structure of the delta opioid receptor bound to naltrindole, Nature 485 (2012) 400–404, http://dx.doi.org/10.1038/nature11111.

[74] N. Eswar, B. John, N. Mirkovic, A. Fiser, V.A. Ilyin, U. Pieper, A.C. Stuart, M.A. Marti-Renom, M.S. Madhusudhan, B. Yerkovich, A. Sali, Tools for comparative protein structure modeling and analysis, Nucleic Acids Res. 31 (13) (2003) 3375–3380, http://dx.doi.org/10.1093/nar/gkg543.

[75] M. Waldherr-Teschner, T. Goetze, W. Heiden, M. Knoblauch, H. Vollhardt, J. Brickmann, Molcad—computer aided visualization and manipulation of models in molecular science, in: Advances in Scientific Visualization, Springer, 1992, pp. 58–67.

[76] P. Li, K.M. Merz, Mcpb.py: A python based metal center parameter builder, J. Chem. Inf. Model. 56 (4) (2016) 599–604, http://dx.doi.org/10.1021/acs.jcim.5b00674.

[77] D. Case, K. Belfon, I. Ben-Shalom, S. Brozell, D. Cerutti, T. Cheatham, V. Cruzeiro, T. Darden, R. Duke, G. Giambasu, et al., Amber2020, University of California, San Fransisco, J. Amer. Chem. Soc. 142 (2020) 3823–3835.

[78] C.R. Groom, I.J. Bruno, M.P. Lightfoot, S.C. Ward, The cambridge structural database, Acta Crystsllogr. B Struct. Sci. Cryst. Eng. Mater. B 72 (2016) 171–179, http://dx.doi.org/10.1107/S2052520616003954.

[79] P. Li, K.M. Merz, Metal ion modeling using classical mechanics, Chem. Rev. 117 (3) (2017) 1564–1686, http://dx.doi.org/10.1021/acs.chemrev.6b00440.

[80] S. Jo, T. Kim, V.G. Iyer, W. Im, Charmm-gui: a web-based graphical user interface for charmm, J. Comput. Chem. 29 (11) (2008) 1859–1865.

[81] C. Bouysset, S. Fiorucci, Prolif: a library to encode molecular interactions as fingerprints, J. Cheminform. 13 (2021) 72, http://dx.doi.org/10.1186/s13321-021-00548-6.

[82] Q. Zeng, L. Ou, W. Wang, D.-Y. Guo, Gastrin, cholecystokinin, signaling, and biological activities in cellular processes, J. Chem. Inf. Model. 11 (2020) 112, http://dx.doi.org/10.3389/fendo.2020.00112.

[83] X. Zhang, C. He, M. Wang, Q. Zhou, D. Yang, Y. Zhu, W. Feng, H. Zhang, A. Dai, X. Chu, J. Wang, Z. Yang, Y. Jiang, U. Sensfuss, Q. Tan, S. Han, S. Reedtz-Runge, H.E. Xu, S. Zhao, M.-W. Wang, B. Wu, Q. Zhao, Structures of the human cholecystokinin receptors bound to agonists and antagonists, Nat. Chem. Biol. 17 (2021) 1230–1237, http://dx.doi.org/10.1038/s41589-021-00866-8.

[84] Y. Ding, H. Zhang, Y.-Y. Liao, L.-N. Chen, S.-Y. Ji, J. Qin, C. Mao, D.-D. Shen, L. Lin, H. Wang, Y. Zhang, X.-M. Li, Structural insights into human brain–gut peptide cholecystokinin receptors, Cell Discov. 5 (2022) 55, http://dx.doi.org/10.1038/s41421-022-00420-3.

[85] A. Waterhouse, M. Bertoni, S. Bienert, G. Studer, G. Tauriello, R. Gumienny, F.T. Heer, T.A.P. de Beer, C. Rempfer, L. Bordoli, R. Lepore, T. Schwede, Swiss-model: homology modelling of protein structures and complexes, Nucleic Acids Res. 46 (Web Server issue) (2018) W296–W303, http://dx.doi.org/10.1093/nar/gky427.

[86] O. Trott, A.J. Olson, Autodock vina: improving the speed and accuracy of docking with a new scoring function, efficient optimization and multithreading, J. Comput. Chem. 31 (2) (2010) 455–641, http://dx.doi.org/10.1002/jcc.21334.

[87] L. Baratto, H. Duan, H. Mäcke, A. Iagaru, Imaging the distribution of gastrin-releasing peptide receptors in cancer, J. Nucl. Med. 61 (6) (2020) 792–798.

[88] H. l. Sun, Q. y. Ma, H. g. Bian, X. m. Meng, J. Jin, Novel insight on grp/grpr axis in diseases, Biomed. Pharmacother. 161 (2023) 114497.

[89] N. Scott, E. Millward, E. Cartwright, S. Preston, P. Coletta, Gastrin releasing peptide and gastrin releasing peptide receptor expression in gastrointestinal carcinoid tumours, J. Clin. Pathol. 57 (2) (2004) 189–192.

[90] A. Hirooka, M. Hamada, D. Fujiyama, K. Takanami, Y. Kobayashi, T. Oti, Y. Katayama, T. Sakamoto, H. Sakamoto, The gastrin-releasing peptide/bombesin system revisited by a reverse-evolutionary study considering xenopus, Sci. Rep. 11 (2021) 13315, http://dx.doi.org/10.1038/s41598-021-92528-x.

[91] H. Zhang, L. Qi, Y. Cai, X. Gao, Gastrin-releasing peptide receptor (grpr) as a novel biomarker and therapeutic target in prostate cancer, Ann. Med. 56 (1) (2024) 2320301, http://dx.doi.org/10.1080/07853890.2024.2320301.

[92] C. Hong, N.J. Byrne, B. Zamlynny, S. Tummala, L. Xiao, J.M. Shipman, A.T. Partridge, C. Minnick, M.J. Breslin, M.T. Rudd, S.J. Stachel, V.L. Rada, J.C. Kern, K.A. Armacost, S.A. Hollingsworth, J.A. O'Brien, D.L. Hall, T.P. McDonald, C. Strickland, A. Brooun, S.M. Soisson, K. Hollenstein, Structures of active-state orexin receptor 2 rationalize peptide and small-molecule agonist recognition and receptor activation, Nat. Commun. 12 (2021) http://dx.doi.org/10.1038/s41467-021-21087-6, 815–815.

[93] S. L. N. Y. (NY), Schrödinger release 2025-1: Maestro, 2025.

[94] R. Franco, I. Reyes-Resina, G. Navarro, Dopamine in health and disease: Much more than a neurotransmitter, Biomedicines 9 (2) (2021) 109, http://dx.doi.org/10.3390/biomedicines9020109.

[95] I. Kawahata, D.I. Finkelstein, K. Fukunaga, Dopamine d1–d5 receptors in brain nuclei: Implications for health and disease, Receptors 3 (2) (2024) 155–181, http://dx.doi.org/10.3390/receptors3020009.

[96] B. M., R. U.F., G. M, P. M.A.S., D. A, M. O, Z. V., Swissdock 2024: major enhancements for small-molecule docking with attracting cavities and autodock vina, Nucleic Acids Res. 52 (W1) (2024) W324–W332, http://dx.doi.org/10.1093/nar/gkae300.

[97] N. Schmid, A.P. Eichenberger, A. Choutko, S. Riniker, M. Winger, A.E. Mark, W.F. van Gunsteren, Definition and testing of the gromos force-field versions 54a7 and 54b7, Eur. Biophys. J. 40 (2011) 843–856, http://dx.doi.org/10.1007/s00249-011-0700-9.

[98] L.W. Chung, W.M.C. Sameera, R. Ramozzi, A.J. Page, M. Hatanaka, G.P. Petrova, T.V. Harris, X. Li, Z. Ke, F. Liu, H.-B. Li, L. Ding, K. Morokuma, The oniom method and its applications, Chem. Rev. 115 (12) (2015) 5678–5796, http://dx.doi.org/10.1021/cr5004419.

[99] M.J. Frisch, G.W. Trucks, H.B. Schlegel, G.E. Scuseria, M.A. Robb, J.R. Cheeseman, G. Scalmani, V. Barone, G.A. Petersson, H. Nakatsuji, X. Li, M. Caricato, A.V. Marenich, J. Bloino, B.G. Janesko, R. Gomperts, B. Mennucci, H.P. Hratchian, J.V. Ortiz, A.F. Izmaylov, J.L. Sonnenberg, D. Williams-Young, F. Ding, F. Lipparini, F. Egidi, J. Goings, B. Peng, A. Petrone, T. Henderson, D. Ranasinghe, V.G. Zakrzewski, J. Gao, N. Rega, G. Zheng, W. Liang, M. Hada, M. Ehara, K. Toyota, R. Fukuda, J. Hasegawa, M. Ishida, T. Nakajima, Y. Honda, O. Kitao, H. Nakai, T. Vreven, K. Throssell, J.A. Montgomery, Jr., J.E. Peralta, F. Ogliaro, M.J. Bearpark, J.J. Heyd, E.N. Brothers, K.N. Kudin, V.N. Staroverov, T.A. Keith, R. Kobayashi, J. Normand, K. Raghavachari, A.P. Rendell, J.C. Burant, S.S. Iyengar, J. Tomasi, M. Cossi, J.M. Millam, M. Klene, C. Adamo, R. Cammi, J.W. Ochterski, R.L. Martin, K. Morokuma, O. Farkas, J.B. Foresman, D.J. Fox, Gaussian 16 Revision C.01, Gaussian Inc. Wallingford CT, 2016.

[100] S. Vangveravong, E. McElveen, M. Taylor, J. Xu, Z. Tu, R.R. Luedtke, R.H. Mach, Synthesis and characterization of selective dopamine d2 receptor antagonists, Bioorg. Med. Chem. 14 (3) (2006) 815–825, http://dx.doi.org/10.1016/j.bmc.2005.09.008.

[101] Q. Wang, R.H. Mach, R.R. Luedtke, D.E. Reichert, Subtype selectivity of dopamine receptor ligands: Insights from structure and ligand-based methods, J. Chem. Inf. Model. 50 (11) (2010) 1970–1985, http://dx.doi.org/10.1021/ci1002747.

[102] S. Wang, T. Che, A. Levit, B.K. Shoichet, D. Wacker, B.L. Roth, Structure of the d2 dopamine receptor bound to the atypical antipsychotic drug risperidone, Nature 555 (2018) 269–273, http://dx.doi.org/10.1038/nature25758.

[103] J. Yin, K.-Y.M. Chen, M.J. Clark, M. Hijazi, P. Kumari, X. chen Bai, R.K. Sunahara, P. Barth, D.M. Rosenbaum, Structure of a d2 dopamine receptor–g-protein complex in a lipid membrane, Nature 584 (2020) 125–129, http://dx.doi.org/10.1038/s41586-020-2379-5.

[104] E.Y.T. Chien, W. Liu, Q. Zhao, V. Katritch, G.W. Han, M.A. Hanson, L. Shi, A.H. Newman, J.A. Javitch, V. Cherezov, R.C. Stevens, Structure of the human dopamine d3 receptor in complex with a d2/d3 selective antagonist, Science 330 (6007) (2010) 1091–1095, http://dx.doi.org/10.1126/science.1197410.

[105] P. Xu, S. Huang, C. Mao, B.E. Krumm, X.E. Zhou, Y. Tan, X.-P. Huang, Y. Liu, D.-D. Shen, Y. Jiang, X. Yu, H. Jiang, K. Melcher, B.L. Roth, X. Cheng, Y. Zhang, H.E. Xu, Structures of the human dopamine d3 receptor-gi complexes, Mol. Cell. 81 (6) (2021) http://dx.doi.org/10.1016/j.molcel.2021.01.003, 1147–1159.e4.

[106] G. Jones, P. Willett, R.C. Glen, A.R. Leach, R. Taylor, Development and validation of a genetic algorithm for flexible docking, J. Mol. Biol. 267 (3) (1997) 727–748.

[107] M.E. Bianchi, R. Mezzapelle, The chemokine receptor cxcr4 in cell proliferation and tissue regeneration, Front. Immunol. 11 (2020) 2109, http://dx.doi.org/10.3389/fimmu.2020.02109.

[108] J. Vagner, H.L. Handl, Y. Monguchi, U. Jana, L.J. Begay, E.A. Mash, V.J. Hruby, R.J. Gillies, Rigid linkers for bioactive peptides, Bioconjugate Chem. 17 (6) (2006) 1545–1550, http://dx.doi.org/10.1021/bc060154p.

[109] B. Wu, E.Y.T. Chien, C.D. Mol, G. Fenalti, W. Liu, V. Katritch, R. Abagyan, A. Brooun, P. Wells, F.C. Bi, D.J. Hamel, P. Kuhn, T.M. Handel, V. Cherezov, R.C. Stevens, Structures of the cxcr4 chemokine gpcr with small-molecule and cyclic peptide antagonists, Science 330 (6007) (2010) 1066–1071, http://dx.doi.org/10.1126/science.1194396.

[110] Y. Yang, K. Yao, M.P. Repasky, K. Leswing, R. Abel, B.K. Shoichet, S.V. Jerome, Efficient exploration of chemical space with docking and deep learning, J. Chem. Theory Comput. 17 (11) (2021) 7106–7119.

[111] M.P. Crump, J. Gong, P. Loetscher, K. Rajarathnam, A. Amara, F. Arenzana-Seisdedos, J. Virelizier, M. Baggiolini, B.D. Sykes, I. Clark-Lewis, Solution structure and basis for functional activity of stromal cell-derived factor-1; dissociation of cxcr4 activation from binding and inhibition of hiv-1, EMBO J. 16 (1997) 6996–7007, http://dx.doi.org/10.1093/emboj/16.23.6996.

[112] D.D. Marino, P. Conflitti, S. Motta, V. Limongelli, Structural basis of dimerization of chemokine receptors ccr5 and cxcr4, Nat. Commun. 14 (2023) 6439, http://dx.doi.org/10.1038/s41467-023-42082-z.

[113] G. Van Zundert, J. Rodrigues, M. Trellet, C. Schmitz, P. Kastritis, E. Karaca, A. Melquiond, M. van Dijk, S. De Vries, A. Bonvin, The haddock2. 2 web server: user-friendly integrative modeling of biomolecular complexes, J. Mol. Biol. 428 (4) (2016) 720–725.

[114] D.A. Candito, V. Simov, A. Gulati, S. Kattar, R.W. Chau, B.T. Lapointe, J.L. Methot, D.E. DeMong, T.H. Graham, R. Kurukulasuriya, M.H. Keylor, L. Tong, G.J. Morriello, J.J. Acton, B. Pio, W. Liu, J.D. Scott, M.J. Ardolino, T.A. Martinot, M.L. Maddess, X. Yan, H. Gunaydin, R.L. Palte, S.E. McMinn, L. Nogle, H. Yu, E.C. Minnihan, C.A. Lesburg, P. Liu, J. Su, L.G. Hegde, L.Y. Moy, J.D. Woodhouse, R. Faltus, T. Xiong, P. Ciaccio, J.A. Piesvaux, K.M. Otte, M.E. Kennedy, D.J. Bennett, E.F. DiMauro, M.J. Fell, S. Neelamkavil, H.B. Wood, P.H. Fuller, J.M. Ellis, Discovery and optimization of potent, selective, and brain-penetrant 1-heteroaryl-1 h-indazole lrrk2 kinase inhibitors for the treatment of parkinson's disease, J. Med. Chem. 65 (24) (2022) 16801–16817, http://dx.doi.org/10.1021/acs.jmedchem.3c0112.

[115] Y.T. Pang, Y. Miao, Y. Wang, J.A. McCammon, Gaussian accelerated molecular dynamics in namd, J. Chem. Theory Comput. 132 (1) (2017) 9–19, http://dx.doi.org/10.1021/acs.jctc.6b00931.

[116] T.M. Corneillie, A.J. Fisher, C.F. Meares, Crystal structures of two complexes of the rare-earth-dota-binding antibody 2d12.5: Ligand generality from a chiral system, J. Am. Chem. Soc. 125 (49) (2003) 15039–15048, http://dx.doi.org/10.1021/ja037236y.

[117] D.S. Nørøxe, H.S. Poulsen, U. Lassen, Hallmarks of glioblastoma: a systematic review, ESMO Open 1 (6) (2017) e000144, http://dx.doi.org/10.1136/esmoopen-2016-000144.

[118] L. Rong, N. Li, Z. Zhang, Emerging therapies for glioblastoma: current state and future directions, J. Exp. Clin. Cancer Res. 41 (2022) 142, http://dx.doi.org/10.1186/s13046-022-02349-7.

[119] M.F. Muñoz, S. Argüelles, M. Rosso, R. Medina, R. Coveñas, A. Ayala, M. Muñoz, The neurokinin-1 receptor is essential for the viability of human glioma cells: A possible target for treating glioblastoma, Biomed Res. Int. 2022 (2022) 6291504, http://dx.doi.org/10.1155/2022/6291504.

[120] A.M. Pilip, M. Rius, F. Bruchertseifer, C. Apostolidis, M. Weis, M. Bonelli, M. Laurenza, L. Królicki, A. Morgenstern, In vitro evaluation of^{225}ac-dota-substance p for targeted alpha therapy of glioblastoma multiforme, Biomed Res. Int. 92 (1) (2018) 1344–1356, http://dx.doi.org/10.1111/cbdd.13199.

[121] A.M. MacLeod, K.J. Merchant, M.A. Cascieri, S. Sadowski, E. Ber, C.J. Swain, R. Baker, N-acyl-l-tryptophan benzyl esters: potent substance p receptor antagonists, J. Med. Chem. 36 (14) (1993) 2044–2045, http://dx.doi.org/10.1021/jm00066a015.

[122] G.M. Morris, R. Huey, W. Lindstrom, M.F. Sanner, R.K. Belew, D.S. Goodsell, A.J. Olson, Autodock4 and autodocktools4: Automated docking with selective receptor flexibility, J. Comput. Chem. 30 (16) (2009) 2785–2791.

[123] J. Schöppe, J. Ehrenmann, C. Klenk, P. Rucktooa, M. Schütz, A.S. Doré, A. Plückthun, Crystal structures of the human neurokinin 1 receptor in complex with clinically used antagonists, Nat. Commun. 10 (2019) 17, http://dx.doi.org/10.1038/s41467-018-07939-8.

[124] G. Pándy-Szekeres, C. Munk, T.M. Tsonkov, S. Mordalski, K. Harpsøe, A.S. Hauser, A.J. Bojarski, D.E. Gloriam, Gpcrdb in 2018: adding gpcr structure models and ligands, Nucleic Acids Res. 46 (D1) (2018) D440–D446.

[125] A. Reiner, J. Levitz, Glutamatergic signaling in the central nervous system: Ionotropic and metabotropic receptors in concert, Neuron 98 (6) (2018) 1080–1098, http://dx.doi.org/10.1016/j.neuron.2018.05.018.

[126] R. Crupi, D. Impellizzeri, S. Cuzzocrea, Role of metabotropic glutamate receptors in neurological disorders, Front. Mol. Neurosci. 12 (2019) 20, http://dx.doi.org/10.3389/fnmol.2019.00020.

[127] J.M. Mehnert, A.W. Silk, J.H. Lee, L. Dudek, B.-S. Jeong, J. Li, J.M. Schenkel, E. Sadimin, M. Kane, H. Lin, W.J. Shih, A. Zloza, S. Chen, J.S. Goydos, A phase ii trial of riluzole, an antagonist of metabotropic glutamate receptor 1 (grm1) signaling, in patients with advanced melanoma, Cell Rep. Med. 31 (4) (2018) 534–540, http://dx.doi.org/10.1111/pcmr.12694.

[128] H. Wu, C. Wang, K.J. Gregory, G.W. Han, H.P. Cho, Y. Xia, C.M. Niswender, V. Katritch, J. Meiler, V. Cherezov, P.J. Conn, R.C. Stevens, Structure of a class c gpcr metabotropic glutamate receptor 1 bound to an allosteric modulator, Science 344 (6179) (2014) 58–64, http://dx.doi.org/10.1126/science.1249489.

[129] C. C. G. Inc, Molecular operating environment (moe), chemical computing group inc 1010, 2016.

[130] W. Humphrey, A. Dalke, K. Schulten, Vmd: visual molecular dynamics, J. Mol. Graph. 14 (1) (1996) 33–38.

[131] H. Land, M.S. Humble, Yasara: A tool to obtain structural guidance in biocatalytic investigations, Methods Mol. Biol. 1685 (2018) 43–67.

[132] N. Kunishima, Y. Shimada, Y. Tsuji, T. Sato, M. Yamamoto, T. Kumasaka, S. Nakanishi, H. Jingami, K. Morikawa, Structural basis of glutamate recognition by a dimeric metabotropic glutamate receptor, Nature 407 (6807) (2000) 971–977, http://dx.doi.org/10.1038/35039564.

[133] A. Koehl, H. Hu, D. Feng, B. Sun, Y. Zhang, M.J. Robertson, M. Chu, T.S. Kobilka, E. Pardon, J. Steyaert, J. Tarrasch, S. Dutta, R. Fonseca, W.I. Weis, J.M. Mathiesen, G. Skiniotis, B.K. Kobilka, Structural insights into metabotropic glutamate receptor activation, Nature 566 (7742) (2019) 7984, http://dx.doi.org/10.1038/s41586-019-0881-4.

[134] K. Zhu, X. Yang, H. Tai, X. Zhong, T. Luo, H. Zheng, Her2-targeted therapies in cancer: a systematic review, Biomark. Res. 12 (2024) 16, http://dx.doi.org/10.1186/s40364-024-00565-1.

[135] S.M. Swain, M. Shastry, E. Hamilton, Targeting her2-positive breast cancer: advances and future directions, Nat. Rev. Drug Discov. 22 (2023) 101–126, http://dx.doi.org/10.1038/s41573-022-00579-0.

[136] L. Gandullo-Sánchez, A. Ocaña, A. Pandiella, Her3 in cancer: from the bench to the bedside, J. Exp. Clin. Cancer Res. 41 (2022) 310, http://dx.doi.org/10.1186/s13046-022-02515-x.

[137] H.-S. Cho, K. Mason, K.X. Ramyar, A.M. Stanley, S.B. Gabelli, D.W.D. Jr., D.J. Leahy, Structure of the extracellular region of her2 alone and in complex with the herceptin fab, Nature 421 (2003) 756–760, http://dx.doi.org/10.1038/nature01392.

[138] C. Wang, D. Greene, L. Xiao, R. Qi, R. Luo, Recent developments and applications of the mmpbsa method, Front. Mol. Biosci. 4 (2018) 87, http://dx.doi.org/10.3389/fmolb.2017.00087.

[139] T. Ishikawa, M. Seto, H. Banno, Y. Kawakita, M. Oorui, T. Taniguchi, Y. Ohta, T. Tamura, A. Nakayama, H. Miki, H. Kamiguchi, T. Tanaka, N. Habuka, S. Sogabe, J. Yano, K. Aertgeerts, K. Kamiyama, Design and synthesis of novel human epidermal growth factor receptor 2 (her2)/epidermal growth factor receptor (egfr) dual inhibitors bearing a pyrrolo[3, 2-d]pyrimidine scaffold, J. Med. Chem. 54 (23) (2011) 8030–8050, http://dx.doi.org/10.1021/jm2008634.

[140] R. Kumari, R. Kumar, A. Lynn, g_mmpbsa—a gromacs tool for high-throughput mm-pbsa calculations, J. Chem. Inf. Model. 54 (7) (2014) 1951–1962, http://dx.doi.org/10.1021/ci500020m.

[141] Y. Gu, B. Dong, X. He, Z. Qiu, J. Zhang, M. Zhang, H. Liu, X. Pang, Y. Cui, The challenges and opportunities of $\alpha v\beta 3$-based therapeutics in cancer: From bench to clinical trials, Pharmacol. Res. 189 (2023) 106694, http://dx.doi.org/10.1016/j.phrs.2023.106694.

[142] J.-P. Xiong, T. Stehle, R. Zhang, A. Joachimiak, M. Frech, S.L. Goodman, M.A. Arnaout, Crystal structure of the extracellular segment of integrin $\alpha v\beta 3$ in complex with an arg-gly-asp ligand, Science 296 (5565) (2002) 151–155, http://dx.doi.org/10.1126/science.1069040.

[143] S.J. Archibald, L. Allott, The aluminium-[18f]fluoride revolution: simple radiochemistry with a big impact for radiolabelled biomolecules, EJNMMI Radiopharm. Chem. 6 (2021) 30, http://dx.doi.org/10.1186/s41181-021-00141-0.

[144] T. Arimori, N. Miyazaki, E. Mihara, M. Takizawa, Y. Taniguchi, C. Cabañas, K. Sekiguchi, J. Takagi, Structural mechanism of laminin recognition by integrin, Nat. Commun. 12 (2021) 4012, http://dx.doi.org/10.1038/s41467-021-24184-8.

[145] S. Singh, H. Singh, A. Tuknait, K. Chaudhary, B. Singh, S. Kumaran, G.P.S. Raghava, Pepstrmod: structure prediction of peptides containing natural, non-natural and modified residues, Biol. Direct 10 (2015) 73, http://dx.doi.org/10.1186/s13062-015-0103-4.

[146] B.G. Pierce, K. Wiehe, H. Hwang, B.-H. Kim, T. Vreven, Z. Weng, Zdock server: interactive docking prediction of protein–protein complexes and symmetric multimers, Bioinformatics 30 (12) (2014) 1771–1773, http://dx.doi.org/10.1093/bioinformatics/btu097.

[147] Y. Lee, Y. Park, H. Nam, J.-W. Lee, S.-W. Yu, Translocator protein (tspo): the new story of the old protein in neuroinflammation, BMB Rep. 53 (1) (2020) 20–27, http://dx.doi.org/10.5483/BMBRep.2020.53.1.273.

[148] S. Salerno, M. Viviano, E. Baglini, V. Poggetti, D. Giorgini, J. Castagnoli, E. Barresi, S. Castellano, F.D. Settimo, S. Taliani, Tspo radioligands for neuroinflammation: An overview, Molecules 29 (17) (2024) 4212, http://dx.doi.org/10.3390/molecules29174212.

[149] L. Ma, H. Zhang, N. Liu, P. qi Wang, W. zhi Guo, Q. Fu, L. bo Jiao, Y. qun Ma, W.-D. Mi, Tspo ligand pk11195 alleviates neuroinflammation and beta-amyloid generation induced by systemic lps administration, Brain Res. Bull. 121 (2016) 192–200, http://dx.doi.org/10.1016/j.brainresbull.2016.02.001.

[150] C.Y. Chan, Z. Chen, F. Guibbal, G. Dias, G. Destro, E. O'Neill, M. Veal, D. Lau, M. Mosley, T.C. Wilson, V. Gouverneur, B. Cornelissen, [^{123}i]cc1: A parp-targeting, auger electron–emitting radiopharmaceutical for radionuclide therapy of cancer, J. Nucl. Med. 66 (2) (2025) 1–7, http://dx.doi.org/10.2967/jnumed.123.265429.

[151] M. Mehta, A. Adem, M. Sabbagh, New acetylcholinesterase inhibitors for alzheimer's disease, Int. J. Alzheimer's Dis. 2012 (1) (2012) 1–8, http://dx.doi.org/10.1155/2012/728983.

[152] A.P. Jaswal, P.P. Hazari, S. Prakash, P. Sethi, A. Kaushik, B.G. Roy, S. Kathait, B. Singh, A.K. Mishra, [^{99m}Tc]tc-dtpa-bis(cholineethylamine) as an oncologic tracer for the detection of choline transporter (cht) and choline kinase (chk) expression in cancer, ACS Omega 7 (15) (2022) 12509–12523, http://dx.doi.org/10.1021/acsomega.1c04256.

[153] E. Malito, N. Sekulic, W.C.S. Too, M. Konrad, A. Lavie, Elucidation of human choline kinase crystal structures in complex with the products adp or phosphocholine, J. Mol. Biology 364 (2) (2006) 136–151, http://dx.doi.org/10.1016/j.jmb.2006.08.084.

[154] O. B. development team, Open babel 2.4.0, 2016, http://openbabel.org.

[155] X. Wang, W. Liu, K. Li, K. Chen, S. He, J. Zhang, B. Gu, X. Xu, S. Song, Pet imaging of parp expression using^{68}ga-labelled inhibitors, Eur. J. Nucl. Med. Mol. Imaging 50 (2023) 2606–2620, http://dx.doi.org/10.1007/s00259-023-06249-6.

[156] J.M. Dawicki-McKenna, M.-F. Langelier, J.E. DeNizio, A.A. Riccio, C.D. Cao, K.R. Karch, M. McCauley, J.D. Steffen, B.E. Black, J.M. Pascal, Parp-1 activation requires local unfolding of an autoinhibitory domain, Mol. Cell. 60 (5) (2015) 755–768, http://dx.doi.org/10.1016/j.molcel.2015.10.013.

[157] K. Davis, P. Powchick, Tacrine, Lancet 345 (8950) (1995) 625–630, http://dx.doi.org/10.1016/S0140-6736(95)90526-X.

[158] P. Szymański, A. Lázničková, M. Lázniček, M. Bajda, B. Malawska, M. Markowicz, E. Mikiciuk-Olasik, 2 3-dihydro-1h-cyclopenta[b]quinoline derivatives as acetylcholinesterase inhibitors—synthesis, radiolabeling and biodistribution, Int. J. Mol. Sci. 13 (8) (2012) 10067–10090, http://dx.doi.org/10.3390/ijms130810067.

[159] E. Gniazdowska, P. Koźmiński, P. Halik, M. Bajda, K. Czarnecka, E. Mikiciuk-Olasik, K. Masłowska, Z. Rogulski, Ł. Cheda, K. Kilian, P. Szymański, Synthesis, physicochemical and biological evaluation of tacrine derivative labeled with technetium-99 m and gallium-68 as a prospective diagnostic tool for early diagnosis of alzheimer's disease, Bioorg. Chem. 91 (2019) 103136.

[160] Y. Cao, T. Balduf, M.D. Beachy, M.C. Bennett, A.D. Bochevarov, A. Chien, P.A. Dub, K.G. Dyall, J.W. Furness, M.D. Halls, T.F. Hughes, L.D. Jacobson, H.S. Kwak, D.S. Levine, D.T. Mainz, K.B. Moore, M. Svensson, P.E. Videla, M.A. Watson, R.A. Friesner, Quantum chemical package jaguar: A survey of recent developments and unique features, J. Chem. Phys. 161 (5) (2024) 052502, http://dx.doi.org/10.1063/5.0213317.

[161] J. Cheung, M.J. Rudolph, F. Burshteyn, M.S. Cassidy, E.N. Gary, J. Love, M.C. Franklin, J.J. Height, Structures of human acetylcholinesterase in complex with pharmacologically important ligands, J. Med. Chem. 55 (22) (2012) http://dx.doi.org/10.1021/jm300871x, 10282–6.

[162] Y. Nicolet, O. Lockridge, P. Masson, J.C. Fontecilla-Camps, F. Nachon, Crystal structure of human butyrylcholinesterase and of its complexes with substrate and products, J. Biological Chem. 278 (42) (2003) 41141–41147, http://dx.doi.org/10.1074/jbc.M210241200.

[163] M.L. Verdonk, J.C. Cole, M.J. Hartshorn, C.W. Murray, R.D. Taylor, Improved protein-ligand docking using gold, Proteins 52 (4) (2003) 609–623, http://dx.doi.org/10.1002/prot.10465.

[164] S. Debnath, N. Zhou, M. McLaughlin, S. Rice, A.K. Pillai, G. Hao, X. Sun, Psma-targeting imaging and theranostic agents—current status and future perspective, Int. J. Mol. Sci. 23 (3) (2022) 1158, http://dx.doi.org/10.3390/ijms23031158.

[165] M.E. Fakiri, N.M. Geis, N. Ayada, M. Eder, A.-C. Eder, Psma-targeting radiopharmaceuticals for prostate cancer therapy: Recent developments and future perspectives, Cancers 13 (16) (2021) 3967, http://dx.doi.org/10.3390/cancers13163967.

[166] K. Kopka, M. Benešová, C. Bařinka, U. Haberkorn, J. Babich, Glu-ureido-based inhibitors of prostate-specific membrane antigen: Lessons learned during the development of a novel class of low-molecular-weight theranostic radiotracers, J. Nucl. Med. 58 (2) (2017) http://dx.doi.org/10.2967/jnumed.116.186775, 17S–26S.

[167] A.P. Kozikowski, F. Nan, P. Conti, J. Zhang, E. Ramadan, T. Bzdega, B. Wroblewska, J.H. Neale, S. Pshenichkin, J.T. Wroblewski, Design of remarkably simple, yet potent urea-based inhibitors of glutamate carboxypeptidase ii (naaladase), J. Med. Chem. 44 (3) (2001) 298–301, http://dx.doi.org/10.1021/jm000406m.

[168] C. Barinka, Y. Byun, C.L. Dusich, S.R. Banerjee, Y. Chen, M. Castanares, A.P. Kozikowski, R.C. Mease, M.G. Pomper, J. Lubkowski, Interactions between human glutamate carboxypeptidase ii and urea-based inhibitors: Structural characterization, J. Med. Chem. 51 (24) (2008) 7737–7743, http://dx.doi.org/10.1021/jm800765e.

[169] J.R. Mesters, C. Barinka, W. Li, T. Tsukamoto, P. Majer, B.S. Slusher, J. Konvalinka, R. Hilgenfeld, Structure of glutamate carboxypeptidase ii, a drug target in neuronal damage and prostate cancer, EMBO J. 25 (6) (2006) 1375–1384, http://dx.doi.org/10.1038/sj.emboj.7600969.

[170] P.A. Ravindranath, S. Forli, D.S. Goodsell, A.J. Olson, M.F. Sanner, Autodockfr: Advances in protein-ligand docking with explicitly specified binding site flexibility, PLoS Comput. Biol. 11 (12) (2015) e1004586, http://dx.doi.org/10.1074/jbc.M210241200.

[171] E. Mamlins, L. Scharbert, J. Cardinale, M. Krotov, E. Winter, H. Rathke, B. Strodel, A.O. Ankrah, M. Sathekge, U. Haberkorn, C. Kratochwil, F.L. Giesel, The theranostic optimization of psma-gck01 does not compromise the imaging characteristics of [99mtc]tc-psma-gck01 compared to dedicated diagnostic [99mtc]tc-edda/hynic-ipsma in prostate cancer, Mol. Imaging Biol. 26 (2024) 81–89, http://dx.doi.org/10.1007/s11307-023-01881-y.

[172] M.H. Kim, K. Lee, K. Oh, C.H. Kim, H.S. Kil, Y.J. Lee, K.C. Lee, D.Y. Chi, Evaluation of psma target diagnostic pet tracers for therapeutic monitoring of [177lu]ludotadipep of prostate cancer: Screening of psma target efficiency and biodistribution using [18f]dcfpyl and [68ga]psma-11, Biochem. Biophys. Res. Commun. 651 (2023) 107–113, http://dx.doi.org/10.1016/j.bbrc.2023.02.003.

[173] C. Liolios, C. Patsis, G. Lambrinidis, E. Tzortzini, M. Roscher, U. Bauder-Wüst, A. Kolocouris, K. Kopka, Investigation of tumor cells and receptor–ligand simulation models for the development of pet imaging probes targeting psma and grpr and a possible crosstalk between the two receptors, Mol. Pharm. 19 (7) (2022) 2231–2247, http://dx.doi.org/10.1021/acs.molpharmaceut.2c00070.

[174] R. Mukkamala, S.D. Lindeman, K.A. Kragness, I. Shahriar, M. Srinivasaraoa, P.S. Low, Design and characterization of fibroblast activation protein targeted pan-cancer imaging agent for fluorescence-guided surgery of solid tumors, J. Mater. Chem. B 10 (2022) 2038–2046, http://dx.doi.org/10.1039/D1TB02651H.

[175] L. Zhao, F. Kang, Y. Pang, J. Fang, L. Sun, H. Wu, X. Lan, J. Wang, H. Chen, Fibroblast activation protein inhibitor tracers and their preclinical, translational, and clinical status in china, J. Nucl. Med. 65 (1) (2024) http://dx.doi.org/10.2967/jnumed.123.266983, 4S–11S.

[176] L. Juillerat-Jeanneret, P. Tafelmeyer, D. Golshayan, Regulation of fibroblast activation protein-α expression: Focus on intracellular protein interactions, J. Med. Chem. 64 (19) (2021) 14028–14045, http://dx.doi.org/10.1021/acs.jmedchem.1c01010.

[177] R.J. Deutsch-Williams, K.A. Schleyer, R. Das, J.E. Carrothers, R.H. Kohler, C. Vinegoni, R. Weissleder, Fap-targeted fluorescent imaging agents to study cancer-associated fibroblasts in vivo, Bioconjugate Chem. 36 (1) (2025) 44–53, http://dx.doi.org/10.1021/acs.bioconjchem.4c00426.

[178] Y. Luo, P. Zhang, Z. Wu, L. Zou, X. Bai, X. Li, W. Gan, F. Wang, Z. Han, Q. Lin, F. Wang, Y. Gu, 99Mtc-labeled quinolone-based novel skeletal tracers for tumor visualization through fibroblast activation protein, J. Med. Chem. 68 (6) (2025) 6735–6747, http://dx.doi.org/10.1021/acs.jmedchem.5c00132.

[179] K. Saito, H. Watanabe, K. Nakashima, M. Ono, Preclinical characterization of novel fap-2286-based radioligand with albumin binder for improved tumor retention, ACS Med. Chem. Lett. XX (XX) (2025) XX, http://dx.doi.org/10.1021/acsmedchemlett.4c00630.

[180] D. Trujillo-Benítez, M. Luna-Gutiérrez, G. Ferro-Flores, B. Ocampo-García, C. Santos-Cuevas, G. Bravo-Villegas, E. Morales-Ávila, P. Cruz-Nova, L. Díaz-Nieto, J. García-Quiroz, E. Azorín-Vega, A. Rosato, L. Meléndez-Alafort, Design, synthesis and preclinical assessment of 99mtc-ifap for in vivo fibroblast activation protein (fap) imaging, Molecules 27 (1) (2022) 264, http://dx.doi.org/10.3390/molecules27010264.

[181] J.-J. Lin, C.-P. Chuang, J.-Y. Lin, F.-T. Huang, C.-W. Huang, Rational design, pharmacomodulation, and synthesis of [68ga]ga-alb-faptp-01, a selective tumor-associated fibroblast activation protein tracer for pet imaging of glioma, ACS Sens. 6 (9) (2021) 3424–3435, http://dx.doi.org/10.1021/acssensors.1c01316.

[182] L. Meng, J. Fang, L. Zhao, T. Wang, P. Yuan, Z. Zhao, R. Zhuang, Q. Lin, H. Chen, X. Chen, X. Zhang, Z. Guo, Rational design and pharmacomodulation of protein-binding theranostic radioligands for targeting the fibroblast activation protein, J. Med. Chem. 65 (12) (2022) 8245–8257, http://dx.doi.org/10.1021/acs.jmedchem.1c02162.

[183] Y. Wang, H. Yuan, N. Liu, S. Tang, Y. Feng, Y. Liu, P. Cai, L. Xia, W. Zheng, Y. Chen, Z. Zhou, High affinity and fap-targeted radiotracers: A potential design strategy to improve the pharmacokinetics and tumor uptake for fap inhibitors, J. Med. Chem. 66 (13) (2023) 8614–8627, http://dx.doi.org/10.1021/acs.jmedchem.3c00259.

[184] J. Huang, X. Zhang, Q. Liu, F. Gong, Y. Huang, S. Huang, L. Fu, G. Tang, 68Ga/177lu-labeled theranostic pair for targeting fibroblast activation protein with improved tumor uptake and retention, J. Med. Chem. 67 (19) (2024) 17785–17795, http://dx.doi.org/10.1021/acs.jmedchem.4c01812.

[185] K. Zhu, K.W. Borrelli, J.R. Greenwood, T. Day, R. Abel, R.S. Farid, E. Harder, Docking covalent inhibitors: A parameter free approach to pose prediction and scoring, J. Chem. Inf. Model. 54 (7) (2014) 1932–1940, http://dx.doi.org/10.1021/ci500118s.

[186] S. Marletta, N. Fusco, E. Munari, C. Luchini, A. Cimadamore, M. Brunelli, G. Querzoli, M. Martini, E. Vigliar, R. Colombari, I. Girolami, F. Pagni, A. Eccher, Atlas of pd-l1 for pathologists: Indications, scores, diagnostic platforms and reporting systems, J. Pers. Med. 12 (7) (2022) 1073, http://dx.doi.org/10.3390/jpm12071073.

[187] M.M. Zhang, R.Y. Huang, B.R. Beno, E.G. Deyanova, J. Li, G. Chen, M.L. Gross, Epitope and paratope mapping of pd-1/nivolumab by mass spectrometry-based hydrogen-deuterium exchange, cross-linking, and molecular docking, Anal. Chem. 92 (2020) 9086–9094, http://dx.doi.org/10.1021/acs.analchem.0c01291.

[188] M. Badenhorst, A.D. Windhorst, W. Beaino, Navigating the landscape of pd-1/pd-l1 imaging tracers: from challenges to opportunities, Front. Med. 11 (2024) 1401515, http://dx.doi.org/10.3389/fmed.2024.1401515.

[189] A. Parvez, F. Choudhary, P. Mudgal, R. Khan, K.A. Qureshi, H. Farooqi, A. Aspatwar, Pd-1 and pd-l1: architects of immune symphony and immunotherapy breakthroughs in cancer treatment, Front. Immunol. 14 (2023) 1296341, http://dx.doi.org/10.3389/fimmu.2023.1296341.

[190] M. Fan, J. Yao, Z. Zhao, X. Zhang, J. Lu, 99Mtc-labeled cyclic peptide targeting pd-l1 as a novel nuclear imaging probe, Pharmaceutics 17 (7) (2024) 906, http://dx.doi.org/10.3390/ph17070906.

[191] J.J.P. Stewart, Mopac2016, 2016.

[192] N. Komaniecka, S. Maroszek, M. Drozdzik, S. Oswald, M. Drozdzik, Transporter proteins as therapeutic drug targets—with a focus on sglt2 inhibitors, Int. J. Mol. Sci. 25 (13) (2024) 6926, http://dx.doi.org/10.3390/ijms25136926.

[193] N. Carmichael, P.J.R. Day, Cell surface transporters and novel drug developments, Front. Pharmacol. 13 (2022) 852938, http://dx.doi.org/10.3389/fphar.2022.852938.

[194] H. Qosa, L.A. Mohamed, S. Alqahtani, B.S. Abuasal, R.A. Hill, A. Kaddoumi, Transporters as drug targets in neurological diseases, Clin. Pharmacol. Ther. 100 (5) (2016) 441–453, http://dx.doi.org/10.1002/cpt.435.

[195] P.-B. Ancey, C. Contat, E. Meylan, Glucose transporters in cancer - from tumor cells to the tumor microenvironment, FEBS J. 285 (16) (2018) 2926–2943, http://dx.doi.org/10.1111/febs.14577.

[196] M. Pliszka, L. Szablewski, Glucose transporters as a target for anticancer therapy, Cancers 13 (16) (2021) 4184, http://dx.doi.org/10.3390/cancers13164184.

[197] O. Kilicoglu, N. Sepay, E. Ozgenc, E. Gundogdu, U. Kara, S. Alomairy, M.S. Al-Buriahi, Evaluation of f-18 fdg radiopharmaceuticals through molecular docking and radiation effects, Appl. Radiat. Isot. 191 (2023) 110553, http://dx.doi.org/10.1016/j.apradiso.2022.110553.

[198] D. Deng, C. Xu, P. Sun, J. Wu, C. Yan, M. Hu, N. Yan, Crystal structure of the human glucose transporter glut1, Nature 510 (2014) 121–125, http://dx.doi.org/10.1038/nature13306.

[199] N. Nomura, G. Verdon, H.J. Kang, T. Shimamura, Y. Nomura, Y. Sonoda, S.A. Hussien, A.A. Qureshi, M. Coincon, Y. Sato, H. Abe, Y. Nakada-Nakura, T. Hino, T. Arakawa, O. Kusano-Arai, H. Iwanari, T. Murata, T. Kobayashi, T. Hamakubo, M. Kasahara, S. Iwata, D. Drew, Structure and mechanism of the mammalian fructose transporter glut5, Nature 526 (7573) (2015) 397–401, http://dx.doi.org/10.1038/nature14909.

[200] C. Bedart, N. Renault, P. Chavatte, A. Porcherie, A. Lachgar, M. Capron, A. Farce, Sinaps: A software tool for analysis and visualization of interaction networks of molecular dynamics simulations, J. Chem. Inf. Model. 62 (6) (2022) 1425–1436, http://dx.doi.org/10.1021/acs.jcim.1c00854.

[201] B. Nepal, S. Das, M.E. Reith, S. Kortagere, Overview of the structure and function of the dopamine transporter and its protein interactions, Front. Physiol. 14 (2023) 1150355, http://dx.doi.org/10.3389/fphys.2023.1150355.

[202] J. Won, G.Y. Lee, S. Jo, J. Lee, S. Lee, J.S. Kim, C. Sung, J.S. Oh, K.-Y. Kwon, S.B. Park, J. Lee, J. Yum, S.J. Chung, N. Kim, Enhancing 3d dopamine transporter imaging as a biomarker for parkinson's disease via self-supervised learning with diffusion models, Cell Rep. Med. 6 (7) (2025) 102207, http://dx.doi.org/10.1016/j.xcrm.2025.102207.

[203] S. for Molecular Descriptor Calculation, Kode srl, 2025, Dragon, version 7.0.10.

[204] P. Gramatica, S. Cassani, N. Chirico, Qsarins-chem: Insubria datasets and new qsar/qspr models for environmental pollutants in qsarins, J. Comput. Chem. 35 (13) (2014) 1036–1044, http://dx.doi.org/10.1002/jcc.23576.

[205] T.S. Chisholm, M. Mackey, C.A. Hunter, Discovery of high-affinity amyloid ligands using a ligand-based virtual screening pipeline, J. Am. Chem. Soc. 145 (29) (2023) 15936–15950, http://dx.doi.org/10.1021/jacs.3c03749.

[206] R.D. Cramer, D.E. Patterson, J.D. Bunce, Comparative molecular field analysis (comfa). 1. effect of shape on binding of steroids to carrier proteins, J. Am. Chem. Soc. 110 (18) (1988) 5959–5967, http://dx.doi.org/10.1021/ja00226a005.

[207] G. Klebe, U. Abraham, T. Mietzner, Molecular similarity indices in a comparative analysis (comsia) of drug molecules to correlate and predict their biological activity, J. Med. Chem. 37 (24) (1994) 4130–4146, http://dx.doi.org/10.1021/jm00050a010.

[208] M. Schweighauser, Y. Shi, A. Tarutani, F. Kametani, A.G. Murzin, B. Ghetti, T. Matsubara, T. Tomita, T. Ando, K. Hasegawa, S. Murayama, M. Yoshida, M. Hasegawa, S.H.W. Scheres, M. Goedert, Structures of α-synuclein filaments from multiple system atrophy, Nature 585 (2020) 464–469, http://dx.doi.org/10.1038/s41586-020-2317-6.

[209] H. Endo, M. Ono, Y. Takado, K. Matsuoka, M. Takahashi, K. Tagai, Y. Kataoka, K. Hirata, K. Takahata, C. Seki, N. Kokubo, M. Fujinaga, W. Mori, Y. Nagai, K. Mimura, K. Kumata, T. Kikuchi, A. Shimozawa, S.K. Mishra, Y. Yamaguchi, H. Shimizu, A. Kakita, H. Takuwa, H. Shinotoh, H. Shimada, Y. Kimura, M. Ichise, T. Suhara, T. Minamimoto, N. Sahara, K. Kawamura, M.-R. Zhang, M. Hasegawa, M. Higuchi, Imaging α-synuclein pathologies in animal models and patients with parkinson's and related diseases, Neuron 112 (15) (2024) http://dx.doi.org/10.1016/j.neuron.2024.05.006, 2540–2557.e8.

[210] M.D. Tuttle, G. Comellas, A.J. Nieuwkoop, D.J. Covell, D.A. Berthold, K.D. Kloepper, J.M. Courtney, J.K. Kim, A.M. Barclay, A. Kendall, W. Wan, G. Stubbs, C.D. Schwieters, V.M.Y. Lee, J.M. George, C.M. Rienstra, Solid-state nmr structure of a pathogenic fibril of full-length human alpha-synuclein, Nat. Struct. Mol. Biol. 23 (5) (2016) 409–415, http://dx.doi.org/10.1038/nsmb.3194.

[211] N. Aho, G. Groenhof, P. Buslaev, Do all paths lead to rome? how reliable is umbrella sampling along a single path? J. Chem. Theory Comput. 20 (15) (2024) 6674–6686, http://dx.doi.org/10.1021/acs.jctc.4c00134.

[212] S. Kumar, J.M. Rosenberg, D. Bouzida, R.H. Swendsen, P.A. Kollman, The weighted histogram analysis method for free-energy calculations on biomolecules. i. the method, J. Comput. Chem. 13 (8) (1992) 1011–1021, http://dx.doi.org/10.1002/jcc.540130812.

[213] J. Tao, X. Kong, Z. Yang, H. Zhu, Embracing artificial intelligence design for better radiopharmaceuticals, iRADIOLOGY 2 (4) (2024) 412–416, http://dx.doi.org/10.1002/ird3.76.

[214] R. Perez-Lopez, N.G. Laleh, F. Mahmood, J.N. Kather, A guide to artificial intelligence for cancer researchers, Nat. Rev. Cancer 24 (2024) 427–441, http://dx.doi.org/10.1038/s41568-024-00694-7.

[215] R.E. Amaro, J. Åqvist, I. Bahar, F. Battistini, A. Bellaiche, D. Beltran, P.C. Biggin, M. Bonomi, G.R. Bowman, R.A. Bryce, G. Bussi, P. Carloni, D.A. Case, A. Cavalli, C.-E.A. Chang, T. E. C. III, M.S. Cheung, C. Chipot, L.T. Chong, P. Choudhary, G.A. Cisneros, C. Clementi, R. Collepardo-Guevara, P. Coveney, R. Covino, T.D. Crawford, M.D. Peraro, B.L. de Groot, L. Delemotte, M.D. Vivo, J.W. Essex, F. Fraternali, J. Gao, J.L. Gelpí, F.L. Gervasio, F.D. González-Nilo, H. Grubmüller, M.G. Guenza, H.V. Guzman, S. Harris, T. Head-Gordon, R. Hernandez, A. Hospital, N. Huang, X. Huang, G. Hummer, J. Iglesias-Fernández, J.H. Jensen, S. Jha, W. Jiao, W.L. Jorgensen, S.C.L. Kamerlin, S. Khalid, C. Laughton, M. Levitt, V. Limongelli, E. Lindahl, K. Lindorff-Larsen, S. Loverde, M. Lundborg, Y.L. Luo, F.J. Luque, C.I. Lynch, A.D.M. Jr., A. Magistrato, S.J. Marrink, H. Martin, J.A. McCammon, K. Merz, V. Moliner, A.J. Mulholland, S. Murad, A.N. Naganathan, S. Nangia, F. Noe, A. Noy, J. Oláh, M.L. O'Mara, M.J. Ondrechen, J.N. Onuchic, A. Onufriev, S. Osuna, G. Palermo, A.R. Panchenko, S. Pantano, C. Parish, M. Parrinello, A. Perez, T. Perez-Acle, J.R. Perilla, B.M. Pettitt, A. Pietropaolo, J.-P. Piquemal, A.B. Poma, M. Praprotnik, M.J. Ramos, P. Ren, N. Reuter, A. Roitberg, E. Rosta, C. Rovira, B. Roux, U. Rothlisberger, K.Y. Sanbonmatsu, T. Schlick, A.K. Shaytan, C. Simmerling, J.C. Smith, Y. Sugita, K. Świderek, M. Taiji, P. Tao, D.P. Tieleman, I.G. Tikhonova, J. Tirado-Rives, I. Tuñón, M.W. van der Kamp, D. van der Spoel, S. Velankar, G.A. Voth, R. Wade, A. Warshel, V.V. Welborn, S.D. Wetmore, T.J. Wheeler, C.F. Wong, L.-W. Yang, M. Zacharias, M. Orozco, The need to implement fair principles in biomolecular simulations, Nat. Methods 22 (2025) 641–645, http://dx.doi.org/10.1038/s41592-025-02635-0.

[216] J.D. Murray, H. Bennett-Lenane, P.J. O'Dwyer, B.T. Griffin, Establishing a pharmacoinformatics repository of approved medicines: A database to support drug product development, Mol. Pharm. 22 (1) (2025) 408–423, http://dx.doi.org/10.1021/acs.molpharmaceut.4c00991.

[217] Z. Tanoli, U. Seemab, A. Scherer, K. Wennerberg, J. Tang, M. Vähä-Koskela, Exploration of databases and methods supporting drug repurposing: a comprehensive survey, Brief. Bioinform. 22 (2) (2021) 1656–1678, http://dx.doi.org/10.1093/bib/bbaa003.

[218] Y. Shino, H. Kaneko, Improving molecular design with direct inverse analysis of qsar/qspr model, Mol. Inf. 44 (1) (2025) e202400227, http://dx.doi.org/10.1002/minf.202400227.

[219] A.K. Nangia, Molecular tweaking by generative cheminformatics and ligand–protein structures for rational drug discovery, Bioorg. Chem. 153 (2024) 107920, http://dx.doi.org/10.1016/j.bioorg.2024.107920.

[220] D. Balcells, B.B. Skjelstad, tmqm dataset—quantum geometries and properties of 86k transition metal complexes, J. Chem. Inf. Model. 60 (12) (2020) 6135–6146, http://dx.doi.org/10.1021/acs.jcim.0c01041.

[221] A. Pedretti, A. Mazzolari, G. Vistoli, B. Testa, Metaqsar: An integrated database engine to manage and analyze metabolic data, J. Med. Chem. 61 (3) (2018) 1019–1030, http://dx.doi.org/10.1021/acs.jmedchem.7b01473.

[222] S. Gervasoni, G. Malloci, A. Bosin, A.V. Vargiu, H.I. Zgurskaya, P. Ruggerone, Ab-db: Force-field parameters, md trajectories, qm-based data, and descriptors of antimicrobials, Sci. Data 9 (2022) 148, http://dx.doi.org/10.1038/s41597-022-01261-1.

[223] C. Isert, K. Atz, J. Jiménez-Luna, G. Schneider, Qmugs, quantum mechanical properties of drug-like molecules, Sci. Data 9 (2022) 273, http://dx.doi.org/10.1038/s41597-022-01390-7.

[224] T.A. Soares, A. Nunes-Alves, A. Mazzolari, F. Ruggiu, G.-W. Wei, K. Merz, The (re)-evolution of quantitative structure–activity relationship (qsar) studies propelled by the surge of machine learning methods, J. Chem. Inf. Model. 62 (22) (2022) 5317–5320, http://dx.doi.org/10.1021/acs.jcim.2c01422.

[225] F. Bamdi, F. Shiri, S. Ahmadi, M. Salahinejad, F. Bazzi-Allahri, Optimization of monte carlo method-based qspr modeling for lipophilicity in radiopharmaceuticals, Chem. Phys. Lett. 843 (2024) 141239, http://dx.doi.org/10.1016/j.cplett.2024.141239.

[226] G. Chen, Y. Qin, R. Sheng, Integrating prior chemical knowledge into the graph transformer network to predict the stability constants of chelating agents and metal ions, J. Chem. Inf. Model. 64 (15) (2024) 5867–5877, http://dx.doi.org/10.1021/acs.jcim.4c00614.

[227] L.D. Pettit, K.J. Powell, The iupac stability constants database, 2006.

[228] RDKit: open-source cheminformatics, 2013-2024, http://www.rdkit.org.

[229] E. Boros, P. Comba, J.W. Engle, C. Harriswangler, S.E. Lapi, J.S. Lewis, S. Mastroianni, L.M. Mirica, C. Platas-Iglesias, C.F. Ramogida, R. Tripier, M. Tosato, Chemical tools to characterize the coordination chemistry of radionuclides for radiopharmaceutical applications, Chem. Rev. (2025) http://dx.doi.org/10.1021/acs.chemrev.5c00641.

[230] R. Southworth, R.T.M. de Rosales, L.K. Meszaros, M.T. Ma, G.E.D. Mullen, G. Fruhwirth, J.D. Young, C. Imberti, J. Bagunya-Torres, E. Andreozzi, P.J. Blower, Opportunities and challenges for metal chemistry in molecular imaging: from gamma camera imaging to pet and multimodality imaging, Adv. Inorg. Chem. 68 (2018) 1–41, http://dx.doi.org/10.1016/bs.adioch.2015.09.001.

[231] M.J. Salgueiro, M. Zubillaga, Theranostic nanoplatforms in nuclear medicine: Current advances, emerging trends, and perspectives for personalized oncology, J. Nanotheranostics 6 (4) (2025) 27, http://dx.doi.org/10.3390/jnt6040027.

[232] L. Aranda-Lara, M. Trujillo-Nolasco, C.M. López-Marmolejo, K. Cárdenas-Rodríguez, V.O. Gómez-Pulido, E. Morales-Avila, B. Ocampo-García, N.P. Jiménez-Mancilla, J.A. Estrada, G. Otero, K. Isaac-Olivé, Chitosan/sirna complex in mimetic high-density lipoproteins as specific/hybrid transfection technology for sr-b1 expressing cancer cells, J. Drug Deliv. Sci. Technol. 101 (2024) 106274, http://dx.doi.org/10.1016/j.jddst.2024.106274.

[233] E.C. Pratt, T.M. Shaffer, J. Grimm, Nanoparticles and radiotracers: Advances toward radio-nanomedicine, Wiley Interdiscip. Rev. Nanomed. Nanobiotechnol. 8 (6) (2016) 872–890, http://dx.doi.org/10.1002/wnan.1402.

[234] A. Núñez Salinas, C. Parra-Garretón, D. Acuña, S. Peñaloza, G. Günther, S. Bollo, F. Arriagada, J. Morales, Nanoradiopharmaceuticals: Design principles, radiolabeling strategies, and biomedicine applications, Pharmaceutics 17 (7) (2025) 912, http://dx.doi.org/10.3390/pharmaceutics17070912.

[235] A. Ancira-Cortez, N. Jiménez-Mancilla, Mathematical models for optical imaging applications of light emission from $^{177}lu_2o_3$ nanoparticles, Mater. Lett. 402 (2025) 139359, http://dx.doi.org/10.1016/j.matlet.2025.139359.

[236] A. Alalmaie, H.T. Alshahrani, M. Alqahtani, Z. Alshahrani, S. Alahmari, A. Asiri, B. Alqadi, A. Alshahrani, S. Alshahrani, M.H. Akhter, Integrating computational insights in gold nanoparticle-mediated drug delivery: enhancing efficacy and precision, Front. Med. Technol. 7 (2025) 1528826, http://dx.doi.org/10.3389/fmedt.2025.1528826.

[237] X. Gu, Z. Xu, L. Gu, H. Xu, F. Han, B. Chen, X. Pan, Preparation and antibacterial properties of gold nanoparticles: a review, Env. Chem. Lett. 19 (2021) 167–187, http://dx.doi.org/10.1007/s10311-020-01071-0.

[238] P. Hassanzadeh, F. Atyabi, R. Dinarvand, The significance of artificial intelligence in drug delivery system design, Adv. Drug Deliv. Rev. 151–152 (2019) 169–190, http://dx.doi.org/10.1016/j.addr.2019.05.001.